



HAL
open science

Rat anterior cingulate neurons responsive to rule or strategy changes are modulated by the hippocampal theta rhythm and sharp-wave ripples

Mehdi Khamassi, Adrien Peyrache, Karim Benchenane, D. A. Hopkins, N. Lebas, V. Douchamps, J. Droulez, F. P. Battaglia, Sidney Wiener

► To cite this version:

Mehdi Khamassi, Adrien Peyrache, Karim Benchenane, D. A. Hopkins, N. Lebas, et al.. Rat anterior cingulate neurons responsive to rule or strategy changes are modulated by the hippocampal theta rhythm and sharp-wave ripples. *European Journal of Neuroscience*, 2024, pp.1-28. 10.1111/ejn.16496 . hal-04673955

HAL Id: hal-04673955




<https://hal.science/hal-04673955v1>

Submitted on 20 Aug 2024

HAL is a multi-disciplinary open access archive for the deposit and dissemination of scientific research documents, whether they are published or not. The documents may come from teaching and research institutions in France or abroad, or from public or private research centers.

L'archive ouverte pluridisciplinaire **HAL**, est destinée au dépôt et à la diffusion de documents scientifiques de niveau recherche, publiés ou non, émanant des établissements d'enseignement et de recherche français ou étrangers, des laboratoires publics ou privés.

Rat anterior cingulate neurons responsive to rule or strategy changes are modulated by the hippocampal theta rhythm and sharp-wave ripples

M. Khamassi^{1,2}  | A. Peyrache¹ | K. Benchenane¹ | D. A. Hopkins³ |
N. Lebas¹ | V. Douchamps¹  | J. Droulez^{1,2} | F. P. Battaglia^{1,4} | S. I. Wiener¹ 

¹Center for Interdisciplinary Research in Biology (CIRB), Collège de France, CNRS, INSERM, Université PSL, Paris, France

²CNRS, Institute of Intelligent Systems and Robotics, Sorbonne Université, Paris, France

³Department of Medical Neuroscience, Dalhousie University, Halifax, Nova Scotia, Canada

⁴Donders Institute for Brain, Cognition, and Behavior, Radboud Universiteit Nijmegen, Nijmegen, The Netherlands

Correspondence

Sidney Wiener, Center for Interdisciplinary Research in Biology (CIRB), Collège de France, 11 pl. Marcelin Berthelot, 75005 Paris, France.
Email: sidney.wiener@college-de-france.fr

Funding information

This work was supported by Fondation Fyssen (F.P.B.), Fondation pour la Recherche Médicale (A.P.) and EC contracts FP6-IST 027819 (ICEA), FP6-IST-027140 (BACS) and FP6-IST-027017 (NeuroProbes).

Edited by: Clive R Bramhams

Abstract

To better understand neural processing during adaptive learning of stimulus-response-reward contingencies, we recorded synchrony of neuronal activity in anterior cingulate cortex (ACC) and hippocampal rhythms in male rats acquiring and switching between spatial and visual discrimination tasks in a Y-maze. ACC population activity as well as single unit activity shifted shortly after task rule changes or just before the rats adopted different task strategies. Hippocampal theta oscillations (associated with memory encoding) modulated an elevated proportion of rule-change responsive neurons (70%), but other neurons that were correlated with strategy-change, strategy value and reward-rate were not. However, hippocampal sharp wave-ripples modulated significantly higher proportions of rule-change, strategy-change and reward-rate responsive cells during post-session sleep but not pre-session sleep. This suggests an underestimated mechanism for hippocampal mismatch and contextual signals to facilitate ACC to detect contingency changes for cognitive flexibility, a function that is attenuated after it is damaged.

KEYWORDS

goal-directed behaviour, learning, prefrontal cortex, set-shifting, single unit recordings

Abbreviations: A24, A25, and A32, Brodmann areas 24, 25 and 32; ACC, anterior cingulate cortex; ACd, dorsal anterior cingulate cortex; Ccompliant (trial); CA1, subfield 1 of the hippocampus; EM, expectation-maximization (algorithm); FR, firing rate; HPC, hippocampus; IL, infralimbic area; LFP, local field potential; mPFC, medial prefrontal cortex; NC, non-compliant (trial); PETH, peri-event time histogram; PL, prelimbic area; RC, rule change; RC + SC, both rule change and strategy change; REM, rapid eye movement; RR, reward rate; S1, pre-session sleep; S2, post-session sleep; SC, strategy change; SDF, spike density function; SEM, standard error of the mean; SWRs, sharp wave-ripple oscillations.

This is an open access article under the terms of the [Creative Commons Attribution-NonCommercial-NoDerivs](https://creativecommons.org/licenses/by-nc-nd/4.0/) License, which permits use and distribution in any medium, provided the original work is properly cited, the use is non-commercial and no modifications or adaptations are made.

© 2024 The Author(s). *European Journal of Neuroscience* published by Federation of European Neuroscience Societies and John Wiley & Sons Ltd.

1 | INTRODUCTION

Adopting an adaptive behavioural response policy, or strategy, in a novel situation requires observation, deduction and memorization of the rules that govern success as well as failure. Optimizing behaviour in a changing world involves continuous selection of appropriate strategies, as well as desisting from less successful ones. Furthermore, alternative, possibly more beneficial, behavioural strategies should be developed and tested. This all requires tracking outcomes over successive iterations, an application of working memory (Malenka et al., 2009; Yu & Frank, 2015). This would benefit from neural coding for the presence or absence of rewards, which is found in anterior cingulate cortex (ACC) and upstream structures like the hippocampus (HPC; e.g., Hyman et al., 2011; Tabuchi et al., 2003). Furthermore, the HPC is strongly implicated in spatial and contextual coding, but little is known about how hippocampal signal processing modulates neural representations of behavioural flexibility in ACC. Note that the nomenclature here follows van Heukelum et al. (2020): ACC for medial prefrontal cortex (mPFC), A32 for prelimbic area (PL), A25 for infralimbic area (IL) and A24 for anterior cingulate cortices Cg1 and Cg2, also referred to as dorsal anterior cingulate cortex (ACd).

In addition to working memory, ACC and closely associated prefrontal cortex (Arikuni et al., 1994; D'Esposito et al., 1995; Goldman-Rakic, 1987, 1995; Lenartowicz & McIntosh, 2005) mediate other cognitive processes underlying rule-based strategy selection: attention (Shallice, 1988), flexible adaptation of response-selection mechanisms in the presence of novel, fluctuating or ambiguous contexts (Dias et al., 1996; Robbins, 2007) and consolidation of memory (Frankland & Bontempi, 2005). Indeed, patients with damage to prefrontal cortex are impaired in non-cued rule-shifting tasks, showing persistence errors (Drewe, 1974; Milner, 1963). Neurophysiological recordings, as well as neuropsychological studies, indicate a crucial role for the rodent ACC and its primate homologue in encoding task-relevant information such as reward (Pratt & Mizumori, 2001), reward rate (RR) (Genovesio et al., 2005) and action-outcome contingencies (Del Arco et al., 2017; Killcross & Coutureau, 2003). Further, ACC and closely associated areas can represent the current task rule (Bissonette et al., 2013; Chiang et al., 2022; Mansouri et al., 2006; Rich & Shapiro, 2009; but see Malagon-Vina et al., 2018) as well as the behavioural strategy adapted to the current task rule (Durstewitz et al., 2010; Genovesio et al., 2005). Moreover, in tasks involving purely spatial strategies, PFC activity has been reported to shift after instatement of a new rule but before the animal's volitional change in strategy (Karlsson et al., 2012; Powell & Redish, 2016). However, it is unknown whether this result

generalizes to cue-guided strategies, whether distinct PFC populations encode particular types of shifts and how these behavioural flexibility-related prefrontal activities interact with the HPC during behaviour and subsequent sleep.

It is not yet understood how executive and memory functions are linked and coordinated in the HPC-ACC axis. Specifically, how do populations of neurons within the ACC encode different types of task-relevant information in order to both detect sudden rule changes (RCs) and participate in the learning a new behavioural strategy or switching to a previously acquired one following such changes? It is also unclear whether the same ACC neurons are coordinated with HPC during RC detection and during initiation of new behavioural strategies. Furthermore, little is known about such cells' reactivation during sleep in synchrony with hippocampal ripple activity, when memory consolidation would occur (Girardeau et al., 2009). Computational models of strategy selection in the ACC predict that distinct neuronal populations would subserve functions such as reward detection/processing, goal/strategy selection and action planning (Dollé et al., 2018; Hasselmo, 2005; Martinet et al., 2011). Other models suggest that off-line replay may play a critical role in making context- or item-selective activity emerge during learning (e.g., Raudies & Hasselmo, 2014).

A possible substrate for memorizing the outcomes of previous actions in order to detect RCs and implement rewarding strategies could involve synchronization of hippocampal and ACC activity by the theta rhythm, as has been observed during memory tasks (Benchenane et al., 2010; Fries, 2015; Hyman et al., 2005; Jones & Wilson, 2005; O'Neill et al., 2013; Siapas et al., 2005). A mechanism proposed to underlie consolidation of labile hippocampal memory traces into more stable cortical representations invokes the activation of ACC neurons in conjunction with hippocampal oscillations during training sessions. This coordinated activity would then be reactivated in association with hippocampal memory replay during awake and asleep ripples (Jadhav et al., 2016; Peyrache et al., 2009; Tang et al., 2017; Wierzynski et al., 2009; Yu et al., 2018). Sharp wave-ripple oscillation (SWR) activity is coordinated among brain structures, and this is associated with learning (Eschenko et al., 2008; Girardeau et al., 2009; Lansink et al., 2009; Ramadan et al., 2009; Roux, et al., 2017; Tatsuno et al., 2020). Indeed, prefrontal cell assemblies are formed during periods of high HPC-ACC coherence upon initial acquisition of new rules (Benchenane et al., 2010) and are reactivated during SWR in subsequent sleep (Peyrache et al., 2009). Thus, the ACC can be viewed as a neural substrate for learning and evaluating the suitability of action-outcome contingencies (or rules) and orchestrating the execution of appropriate

behavioural strategies (Bunge, 2004), benefitting from hippocampal contextual and memory signals.

In order to reveal neuronal activity profiles that could underlie key prefrontal functions, here we examined single unit activity in ACC subregions A32, A24 and A25 in relation to local field potential (LFP) oscillatory activity in the HPC of rats acquiring and shifting between spatial and cue-guided strategies in a Y-maze (original data set at <https://crcns.org/data-sets/pfc/pfc-6/>). Here, we define the term ‘strategies’ operationally as descriptions of the patterns of behavioural responses relevant to the structure of the task and the maze (see the Supplementary Annex in the [Supporting Information](#)). This term makes no assumptions about the internal representations and neural mechanisms engaged when the animals perform the task. The task was designed to emulate the extradimensional set shifts of the Wisconsin Card Sorting Task employed to diagnose cingulate cortex deficits in human patients (Berg, 1948; Grant et al., 1949; Milner, 1963). Once the rats reached criterion performance in one task, the rule was changed (‘RC sessions’). Then, the animal had to learn that the previous strategy was no longer optimal and had to learn or shift to a new strategy. We examined sessions when the animal changed strategies (‘SC sessions’), and these could include strategies not adherent to the current rule. Individual neurons with firing rate changes in these sessions were identified as RC- or SC- responsive. We examined the modulation of these neurons by the hippocampal theta rhythm (8 Hz) during behaviour, as well as by HPC SWRs during sleep before and after the recording sessions, as these would reflect preferential responsiveness to potentially informative hippocampal signals.

Section 2 will first examine the rats’ behaviour in the binary choice spatial and visual discrimination tasks, then the population dynamics of the anterior cingulate neuronal activity around RCs and strategy changes (SCs, without distinguishing among the individual neurons and averaging activity over entire trials). The next sections examine individual neuronal activity changes during the successive steps of completing the trials, first with parametric statistics, then with Monte Carlo methods. The resulting neurons with identified response types are then compared for firing modulation by hippocampal theta rhythms and sharp wave-ripples.

2 | RESULTS

2.1 | Behaviour

In the Y-maze, each trial began in the start arm. A central barrier was removed, and a cue was lit in the left or right arm in pseudorandom sequence (Figure 1a). To obtain a

liquid reward, the rat had to go to the end of the appropriate reward arm according to the current rule. Learning was by trial and error. Initially, the rewarded arm was on the right side whether it was lit or unlit. The next reward contingencies (RCs) required visits to the lit side (regardless of whether it was to the left or the right), then the left side and then the unlit (‘dark’) side (Figure 1a). A different rule was applied (RC) after the rat reached a criterion level of 10 consecutive rewarded trials (or 11 rewards in the previous 12 trials). This stringent criterion was applied because some rats tended to explore other strategies after initial acquisition, and this assured that the performance level had become rather stable.

The five rats performed a total of 3322 trials over 108 sessions. Two rats succeeded at learning only two of the rules (then recordings had to be stopped for technical reasons), and two others learned three, whereas one rat learned all four and then continued on to make a total of 17 extradimensional (i.e., between spatial and visual discrimination) strategy switches between the four rewarded rules (Figure 1c). Learning the first rule (Right) took 10.2 ± 3.7 (SEM) trials on average, while acquiring the Light rule took much longer, 104.2 ± 50.1 trials. Switching to the Left rule then required 34.3 ± 7.8 trials, and then switching to the Dark rule (only by rat 20) took 319 trials. In most cases, performance did not appear to improve gradually from chance to criterion levels—rather, the animals’ performance levels changed abruptly (Figure 1b; cf., Gallistel et al., 2004). Sometimes animals also spontaneously performed an alternation strategy even though it was not rewarded, and this, as well as Right, Light, Left and Dark, is considered as ‘defined’ strategies hereafter. Trials not included in these sequences are considered as expressing an ‘undefined’ strategy. Note, however, that when a Bayesian descriptive model of the behavioural data tested 256 rule combinations (see the Supplementary Annex in the [Supporting Information](#)), the animals’ strategies could be described in other frameworks, such as persistence to the same path (left or right) or cued arm (lit or unlit), as well as alternation. The [Supplementary Annex](#) explains the choice of the defined strategies for the analyses below.

The task rule was changed in 24 sessions, and in 16 of these, the rats also made at least one SC, that is, extinction (cessation) of the previously rewarded strategy, and/or adoption of another defined strategy, rewarded or not. After RCs, 11.4 ± 8.4 trials were required for the animals to abandon the previous strategy, with the exception of one case where a rat persisted for 280 trials before acquiring the next rule. This suggests that, apart from this exception, the rats did not develop habitual behaviour from overtraining. Rather this is consistent with them executing goal-oriented navigation strategies, for

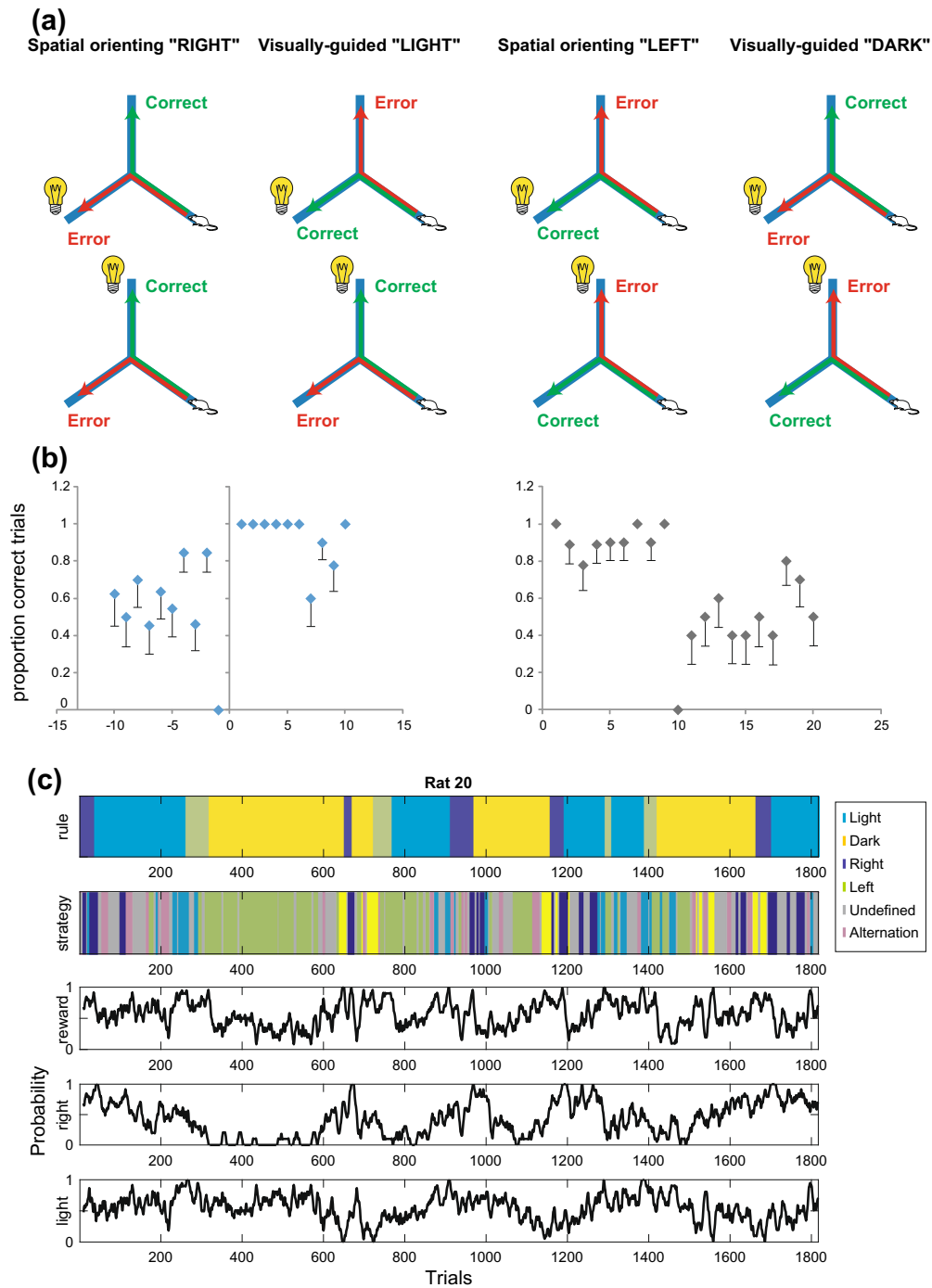


FIGURE 1 Task and behaviour. (a) Schema of the four Y-maze task rules. A visual cue is lit at the end of one of the two reward arms in a pseudo-random sequence. (b) (Left) Reward rate changes upon first acquisition of each rule. The first correct trial is at trial zero. Blue diamond = mean; whiskers = SEM. If no whiskers, SEM = 0. Data are from 13 sessions of initial rule acquisition of various reward contingency rules in the five rats. (Right) Reward rate changes relative to first unrewarded trial that revealed that the task rule has changed (trial number zero). Chance levels of reward after rule change are consistent with initial persistence of the previously rewarded strategy (black diamonds = means; whiskers = SEM). ($n = 10$ sessions). (c) Behaviour in rat 20 over all sessions. Top row: task rule. Second row: strategies used by the animal. The criterion was a minimum of six trials compliant with the strategy. A maximum of 1 non-compliant trial was permitted for 8 compliant trials (permissive criterion; see Section 4 and Supplementary Annex in the [Supporting Information](#)). Third row: probability of reward. Fourth row: probability of going to the right arm. Bottom row: probability of going to the lit arm. Probabilities are calculated as percent of rewarded, right or lit arm choices over sliding windows of 10 trials.

which the HPC-ACC network is implicated (see, e.g., Khamassi & Humphries, 2012). For analyses, the criterion of a minimum of six consecutive trials was selected to define a sequence (or 'block') of trials with a given strategy. Simulations of random choices for this behavioural data set showed that this criterion is sufficient to exclude fortuitous inclusion of stochastic choices (see the Supplementary Annex in the [Supporting Information](#)). The animals followed a defined strategy in 170 blocks that included 2424 trials (for example, see Figure 1c). In a total of 898 trials (27% of all trials), the strategy was classified as undefined. Prior to acquisition of a rewarded task rule, the rats did not tend to simply follow an undefined strategy. Rather, they employed defined strategies other than the currently rewarded one.

The rats changed strategies 118 times, sometimes more than once in a session. Of these, 24 were shifts between the task-relevant spatial and visual strategies (Right, Left, Light or Dark). In 55 cases, rats shifted between a defined and an undefined strategy, and they shifted between a task-relevant strategy and the Alternation strategy 39 times. No spontaneous reversals were observed (that is, between Right and Left or between Light and Dark strategies), nor were they ever rewarded.

In summary, among the 108 recording sessions, the following different types of sessions were recorded (also represented below in Figure 3):

- 6 *RC-only* sessions, when an RC was imposed but the animal made no SC (rather it tended to persist in adhering to the previous rule);
- 65 *SC-only* sessions when an SC occurred (not necessarily to the currently rewarded strategy), but there was no RC;
- 18 *RC+SC* sessions, when at least one SC and one RC event occurred; and
- 19 *Training* sessions, when neither a SC nor a RC occurred.

2.2 | Electrophysiological recordings

The anatomical distribution of the recording sites of the ACC cells is shown in Figure 2. The largest group was located in layer 5 of A32, although layers 2/3 and 6 of A32, and areas A24 and A25 were also represented.

2.3 | Activity transitions at the population level in relation to RC and SC

We first tested if population activity changed relative to RC and SC, as shown previously for criterion

performance in rewarded tasks. Population vectors of activity of simultaneously recorded neurons over the entire trial were compared between each pair of trials in each session to identify those trial(s) when changes in firing rate ('activity transitions') occurred. (Note that this analysis does not distinguish which neurons are most influential in the activity transitions.) Specifically, a (z-scored) population vector correlation matrix was constructed with the element at row i and column j quantifying the correlation between the population vectors at trials i and j (cf. Figure 3). A matrix block decomposition algorithm detected the transition points by searching for the presence of distinct 'sub-matrices' within the matrix. These correspond to sequences of trials with distinct patterns of population activity. This process identified and excluded inter-trial comparisons outside the blocks (e.g., in session 2 of Figure 3, the blue submatrix blocks at the lower left and upper right were excluded) while preserving the maximal amount of information of the matrix (i.e., the highly correlated submatrix blocks at the upper left and lower right of this same session). Block decomposition was performed when the cumulated correlation of off-diagonal terms represented less than 1/3 of the total correlation in the matrix. When a block change occurred, this was considered an activity transition trial.

These resulting transition points correspond to those trials where there is a major change in the population vectors of activity computed from all recorded neurons. These transition trial numbers were then compared with the trial numbers when RC and SC events occurred, and the delays were calculated. This analysis detected neural activity transitions in 100/108 (92.6%) sessions (see examples in Figure 3a). Of these, 81 sessions contained at least one behavioural event (RC or SC). Interestingly, a population activity transition occurred within four trials before or after a behavioural event (either a RC or a SC) in 68 of the 81 sessions (i.e., 84%; Figure 3b). This is more than expected by chance because a Monte Carlo distribution of 1000 population transitions randomly generated in these sessions yielded only 28% of cases with only four or fewer trials between neural and behavioural events (binomial test, $z = 11.0$, $p < .001$). Note, however, that there was also a population activity transition in all 19 Training sessions (where no RC or SC event occurred), consistent with previously reported lability of ACC single neuron activity (e.g., Rich & Shapiro, 2009, p. 7214; 12.6% of their neurons; Tanaka, 2007). This could reflect gradual neural processes underlying acquisition of new rules. (We speculate that this corresponds to our subsample of neurons transitioning between attractor states, and this alone may not be sufficient to alter behaviour. Rather, this might need to be concerted with some critical

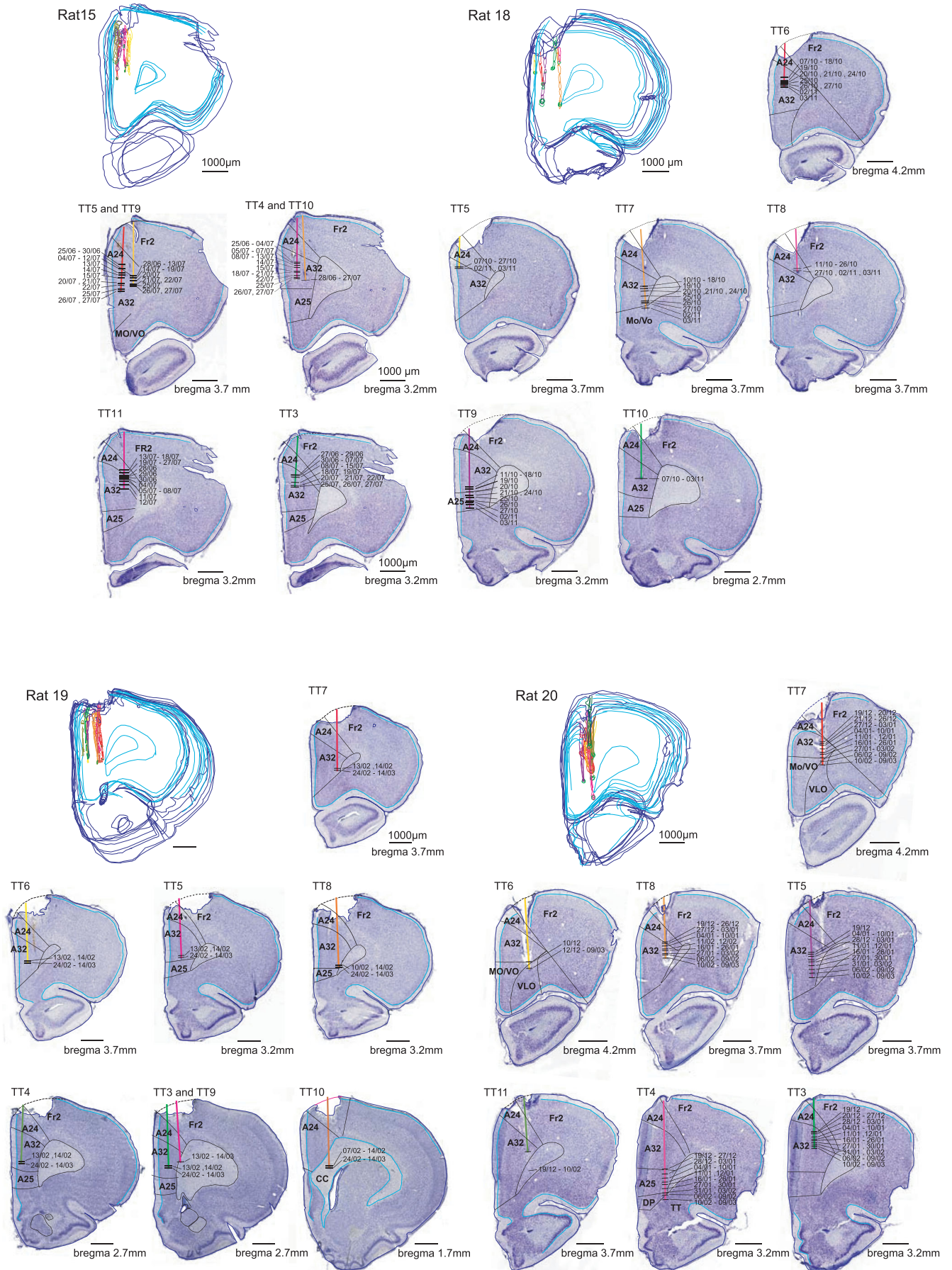


FIGURE 2 Legend on next page.

FIGURE 2 Anatomical localization of recording sites in the rat anterior cingulate cortex (ACC). For each rat, the image to the upper left is a 3D reconstruction of colour-coded tetrode (TT) tracks. The dates (day/month) are indicated for each recording site. The histology for the fifth rat had technical problems and is not shown.

number of other ACC neurons and perhaps in other brain structures as well. Thus, such a population activity pattern could develop over the course of several training sessions as more cells acquire the appropriate behavioural correlate and become synchronous, leading to a behavioural change.) Conversely, in 8 (9%) of the 89 sessions where an RC or SC behavioural event occurred, no neural activity transition was detected in the respective samples of neurons recorded then.

Because multiple behavioural events in the same session could lead to possible confounds, we first examined sessions with only an RC or an SC. In five of the six RC-only sessions, a population vector transition occurred 2.3 ± 1.6 trials (median 2.5 trials) *after* the first trial revealing that the RC had occurred. Thus, this neuronal population activity responded rapidly to the RC, even though no explicit cue was presented to signal the RC's. Strikingly, in the 65 SC-only sessions, the neural activity transition occurred on average $1.0 \pm .86$ trial (median = 1) *before* the first trial of the block of trials beginning with an SC event. Thus, the transitions in ACC population activity tended to anticipate SCs. Analyses of RC + SC sessions were inconclusive with the population vector approach, and these will be examined further below at the single-cell activity level. In summary, the transitions in ACC population activity tended to occur in conjunction with RC or SC events.

In order to examine the relation between hippocampal activity and RC and SC responses in ACC, further analyses focused on single neuron activity modulation by hippocampal theta and SWR. First, however, it was necessary to determine if the population responses also appeared in individual neurons. In contrast with the population activity, the individual neuron analyses distinguish firing rate changes at different points of the maze. This permits reward site activity to be set aside, as this could lead to potential confounds related to changes associated with reward consumption prior to versus after RCs and SCs.

2.4 | Firing rate transitions in single ACC neurons in relation to RC or SC

Of the 2290 recorded ACC neurons, 1888 with average firing rates superior to .3 Hz in at least one of the task periods (pre-start, post-start, pre-arrival at reward site,

post-arrival) were retained for these analyses. Putative interneurons comprised 19% of the cells recorded, and 79% were classified as putative pyramidal cells, and 2% could not be clearly identified. Firstly, 1337 (71%) of the 1888 cells showed behaviourally correlated activity; that is, the firing rate significantly varied across the four trial periods (analysis of variance [ANOVA], $p < .05$). This proportion was similar considering only pyramidal cells as well and also in the subgroup consisting of A32 layer 5 cells. These proportions are compatible with previous reports of data recorded in animals performing other tasks, employing analyses using different analytical criteria (50%: Pratt & Mizumori, 2001; 62%: Mulder et al., 2003; 46%: Rich & Shapiro, 2009).

To provide an overview, neuronal activity was plotted as a function of trials prior to or after RC and SC events. This revealed numerous neurons that appeared to change firing rate relative to these events (Figure 4). These transitions could be either increases or decreases in firing rate after the RC or SC events and occurred in cells with high or low firing rates. To more precisely compare the timing of transitions in firing rates of neurons relative to when RC's and SC's occurred, Monte Carlo analyses (Fujisawa et al., 2008) examined single unit activity along the maze. This only considered maze regions visited on all trials of the session. This analysis first searched for positions on the maze where actual spike activity exceeded shuffled data, first for trials before versus after the 5th trial of the session, then before and after the 6th trial, and so on, seeking the trial that had the greatest difference in average firing before versus after it. These data are represented as the rows of colour raster plots of 2nd column of Figure 5a–e. For example, in a session with 40 trials, one of the random shuffles between trials 1 through 5 and trials 6 through 40 could exchange the sequential bins of trial 1 with that of trial 36, trial 2 with trial 13, trial 3 with trial 40, trial 4 with trial 6 and trial 5 with trial 27. The firing rates in the two surrogate groups were compared for each of the spatial bins, then accumulated with data from other such shuffles to create spike density functions (SDFs) for the shuffled data. Then, analogously to transition detection in the population analysis of Figure 3, the greatest 'peak transition trials' were determined and then compared with the timing of the SC or RC trials. The null hypothesis is that the timing of these peak transition trials is unrelated to these behavioural events.

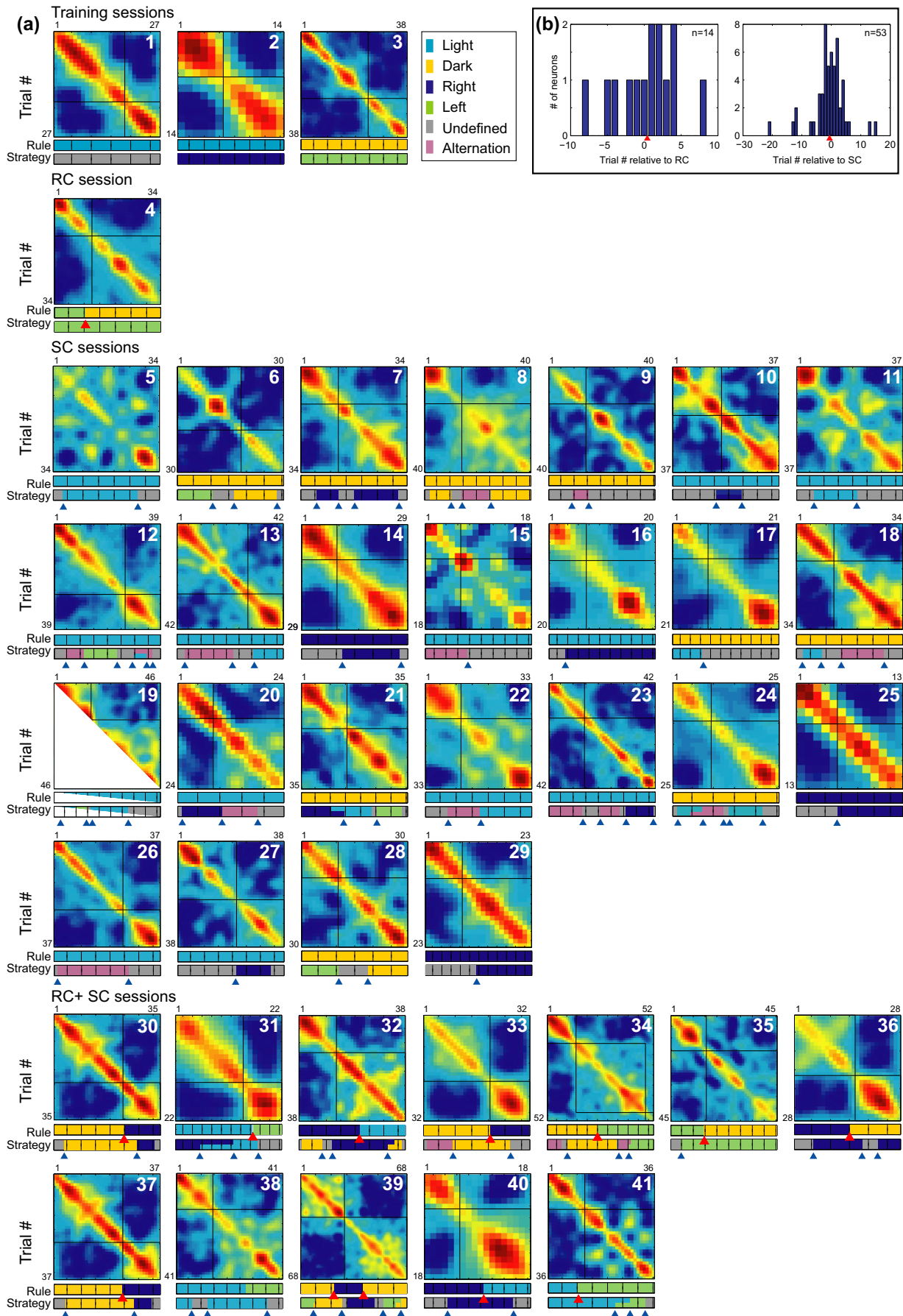


FIGURE 3 Legend on next page.

FIGURE 3 Transitions in population activity over the course of the sessions. (a) Each box plot shows the correlation matrix of the population vectors between different trials (indicated by numbers along the upper and left axes) of example sessions with rule change (RC), strategy change (SC), RC + SC and Training (i.e., with no RC or SC). (Hotter colours indicate higher correlations.) Crossbars represent the automatically determined decomposition of the matrix into sub-blocks along the diagonal. (Examples with no crossbars are presented to demonstrate how subblocks could be absent—in these cases, decomposition led to supra-threshold information loss because off-diagonal terms contained substantial correlations in population activity between trials.) Below the matrices, top bars indicate task rules and, in RC sessions, when they changed (change of bar colour and red arrowheads). Lower bars indicate strategies, and, in cases of SC, the colour of the bar changes (blue arrowheads). Split bars for strategy (e.g., cells 19 and 21) represent trials belonging to both the preceding sequence of trials adherent to one strategy and to the subsequent one adherent to another. (b) Incidence of neurons with shifts in population activity at various delays relative to RC or SC behavioural events (defined to occur at trial zero here). Red arrowheads point to means (SC: $-.36$ trial; RC: $.62$ trial). The animal identifiers and numbers of cells recorded to calculate the population vector for each session are provided in Table 2.

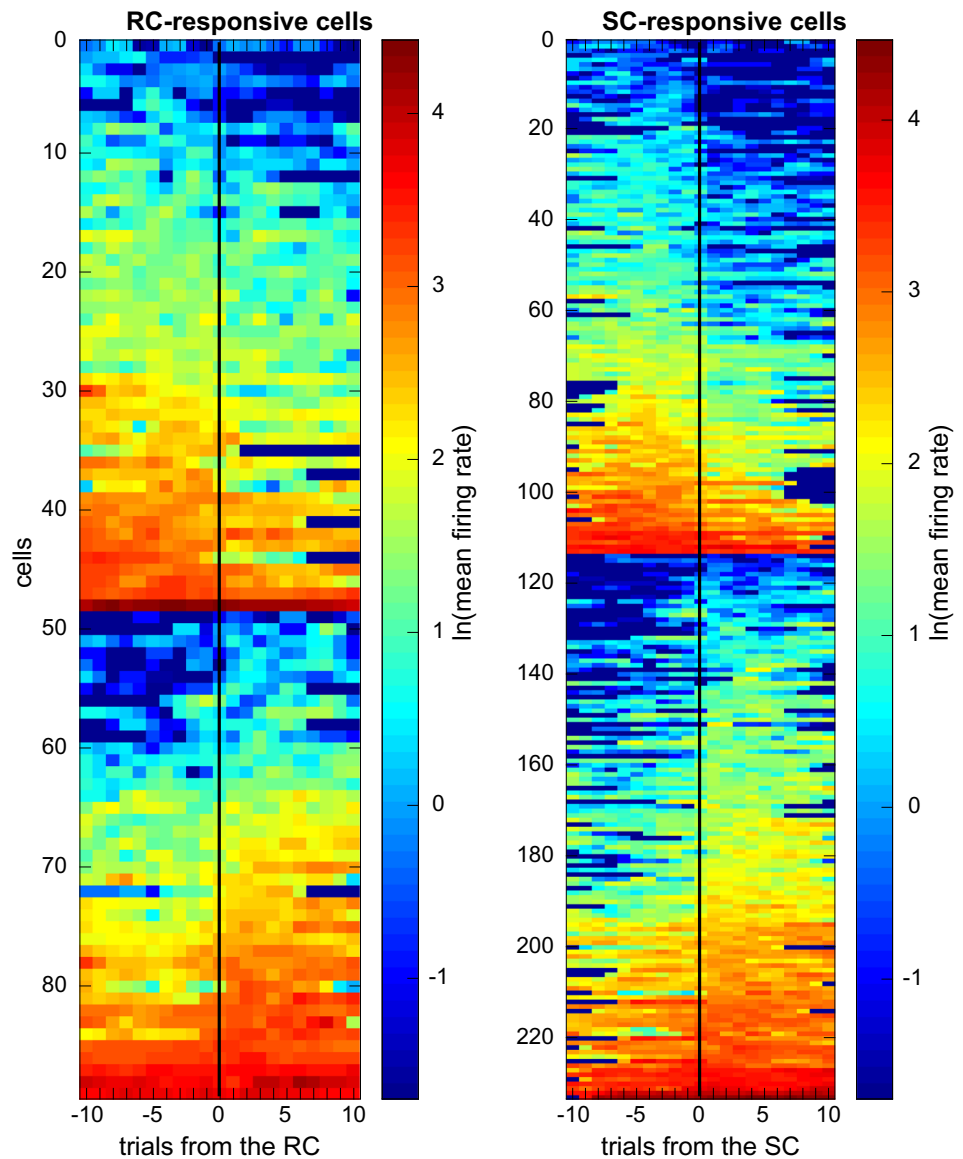


FIGURE 4 Overview of significant firing rate changes in representative individual neurons before and after rule change (RC) and strategy change (SC). Cells with significant decreases in activity are at the top, and those with increases at the bottom. Plots are synchronized so that trial 0 is the one when the RC could be detected by reward absence or the first trial of a run of trials adherent to the new SC.

Among the 114 neurons analysed from the 6 RC-only sessions, 50 (43.9%) showed at least one SDF difference exceeding the shuffled distribution, indicating there was a significant difference in firing rate between at least one of the pairs of blocks of trials in at least one bin on the

maze. Similarly, among the 846 neurons analysed from the 65 SC-only sessions, 400 (47.3%) showed a significant SDF difference (Monte Carlo, $p < .05$, two-tailed). Figures 5a,b shows data from two representative RC-responsive neurons, and Figure 5c–e shows three

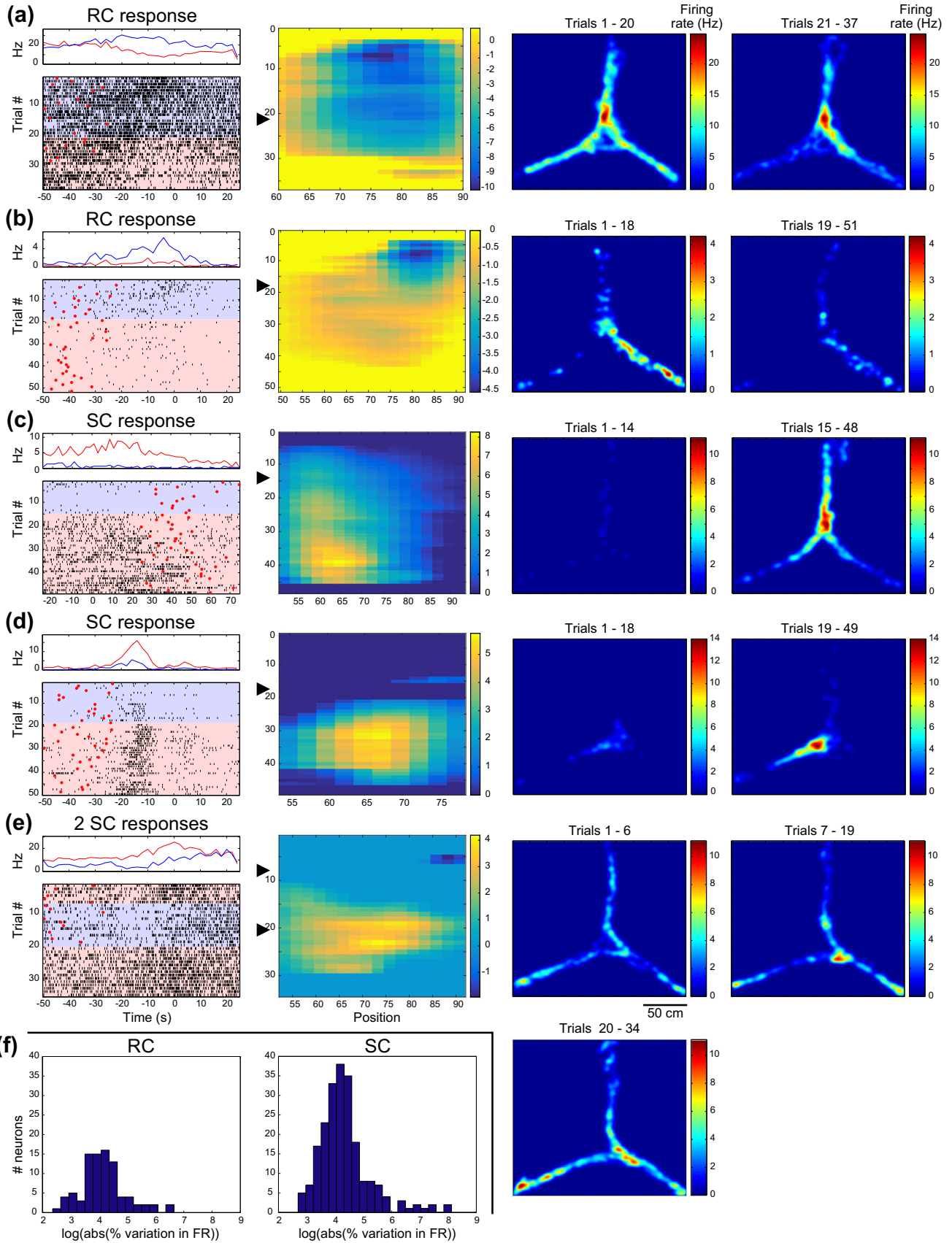


FIGURE 5 Legend on next page.

FIGURE 5 Examples of rule change (RC) and strategy change (SC) associated changes in firing rate. (a–e) Data from representative neurons. The left column contains raster displays and above them, the corresponding histograms of spiking activity, both as functions of time. Blue (or red) histogram traces represent the firing rate before (or after) the RC or SC, corresponding to the colour-coded shading of the raster displays. Each row in the rasters is a single trial. In rasters, when the red circles are after zero, they correspond to reward site arrival, and zero is the trial start event in these cases. When the red circles are before zero, they indicate the trial start events, and zero is the reward site arrival time. (In e, the histogram for trials 1–6 is not shown.) The plots in the second column show all significant Monte Carlo bootstrap spike density function (SDF) values (trial number on y-axis and linearized position on the maze on the x-axis). Only deep blue rectangles (zero) had non-significant SDFs. The colour scale represents the magnitude (in units of spikes/s) of the difference between the SDF value and the upper or lower 2.5% confidence limits. Arrowheads indicate the RC or SC. The third and fourth columns show the spatial distribution of the neuron's activity before and after the RC or SC. The start arm is above. (a) A rule-responsive neuron with stable activity at the decision point and a rule-modulated activity in the arrival arms. (b) A rule-responsive neuron with rule-modulated activity in the left arrival arm. (c) A strategy-responsive neuron with activity selective for the start arm and decision point. (d) A strategy-responsive neuron with activity selective for the decision point and right arrival arm. (e) A strategy-responsive neuron with transitions in activity at two strategy changes on trials #7 and #20 (hence the three spatial plots). The activity is reduced at the decision point while the animal follows the correct Light strategy between trials #7 and #19. The activity remains low during two trials after the task rule change (when the Light strategy is no longer rewarded) but resumes on trial #20 when the rat started a block of Alternation trials. (f) Distribution of the incidence of neurons with respective variations in firing rate following changes in rule (left) or strategy (right). FR = firing rate. X-axis ranges vary among figures because they are limited to maze positions the rats occupied on every trial of the respective sessions.

representative SC-responsive neurons. Figure 5f shows the range of firing rate increases or decreases in comparisons between blocks before versus after the RC or SC.

To detect transitions in single neuron activity, the greatest values of these inter-block differences were determined. Then, for each neuron, the incidences of trials separating blocks with these peak SDF values were plotted as a function of the trial when that session's RC or SC occurred. Because these distributions did not pass the Lilliefors test for normality ($p > .05$; Figure 6a), they were fitted with beta distributions to determine normative values. Strikingly, in Figure 6b, the mean delay was 3.9 ± 2.5 trials after the trial when the RC became evident in RC-only sessions (median = 3 trials after; significantly different from zero, t test, $p < .001$, $n = 8649$). The mean was also 3.8 ± 2.3 trials after the RC for RC + SC sessions (median = 3 trials after, again significantly different from zero, t test, $p < .001$, $n = 9311$).

In SC-only sessions, the mean of the beta distribution of the SDF values was 2.9 ± 1.4 trials before the SC event (Figure 6c; median = 1 trial before; significantly different from zero: t test, $p < .001$, $N = 95,629$). Similarly, in RC + SC sessions, the mean was 2.5 ± 1.3 trials earlier than the SC (median = 1 trial before; t test, $p < .001$). Thus, individual ACC neurons can respond rapidly to changes in action-outcome contingencies (i.e., RC's) or precede adaptive responses to these changes (i.e., SC's). These results are consistent with those of the population analyses (2.3 ± 1.6 trials after RC and $1.0 \pm .86$ trial before SC).

While it seems counter-intuitive that some transitions occur prior to RC (Figures 3b and 6b), this may be related to the lability of ACC neurons or to anticipation of RC by the more experienced rats. The reduced incidence for

separations being observed between blocks for early and for late trials could be related to fewer combinatorial samples there. However, the mean values following RC or preceding SC events cannot be due to these potential confounds.

One possible confound for interpreting RC responses in the spatial discrimination tasks is that the neuronal activity could be correlated with action value, rather than the RC per se. For example, in the Right rule, each trial (rewarded or not) reinforces the value of the appropriate action. This value progresses over trials, but, after RC's, it decreases for the previous rule and increments on each trial with the new rule. There is a similar issue with the visual discrimination rules, and thus, we extended the concept of action value to 'strategy value'. This emulates, in a simple and parsimonious way, the strategy value learning process in relevant computational models (Dollé et al., 2018; see Figure S1). Strikingly, multiple regression analyses showed that the activity of only 8/50 (16%) of RC-responsive neurons was significantly correlated with one of the strategy values ($p < .05$, significance threshold set with bootstrapping with 10,000 shuffles). Thus, most RC responses cannot simply be a confound with strategy value. Interestingly, firing in 288 other neurons was exclusively correlated with strategy value, and their modulation by hippocampal rhythms is discussed below.

Another possible confound concerned reward rate (RR) which could toggle between 100% and 50% after RCs or SCs. But the firing rate of only 4/50 (8%) RC-responsive neurons was correlated with RR ($p < .05$, regression analyses with bootstrapping, with rate averaged over six trials). Similarly, only a minority of SC neurons was significantly correlated with RR (16/400, 4%),

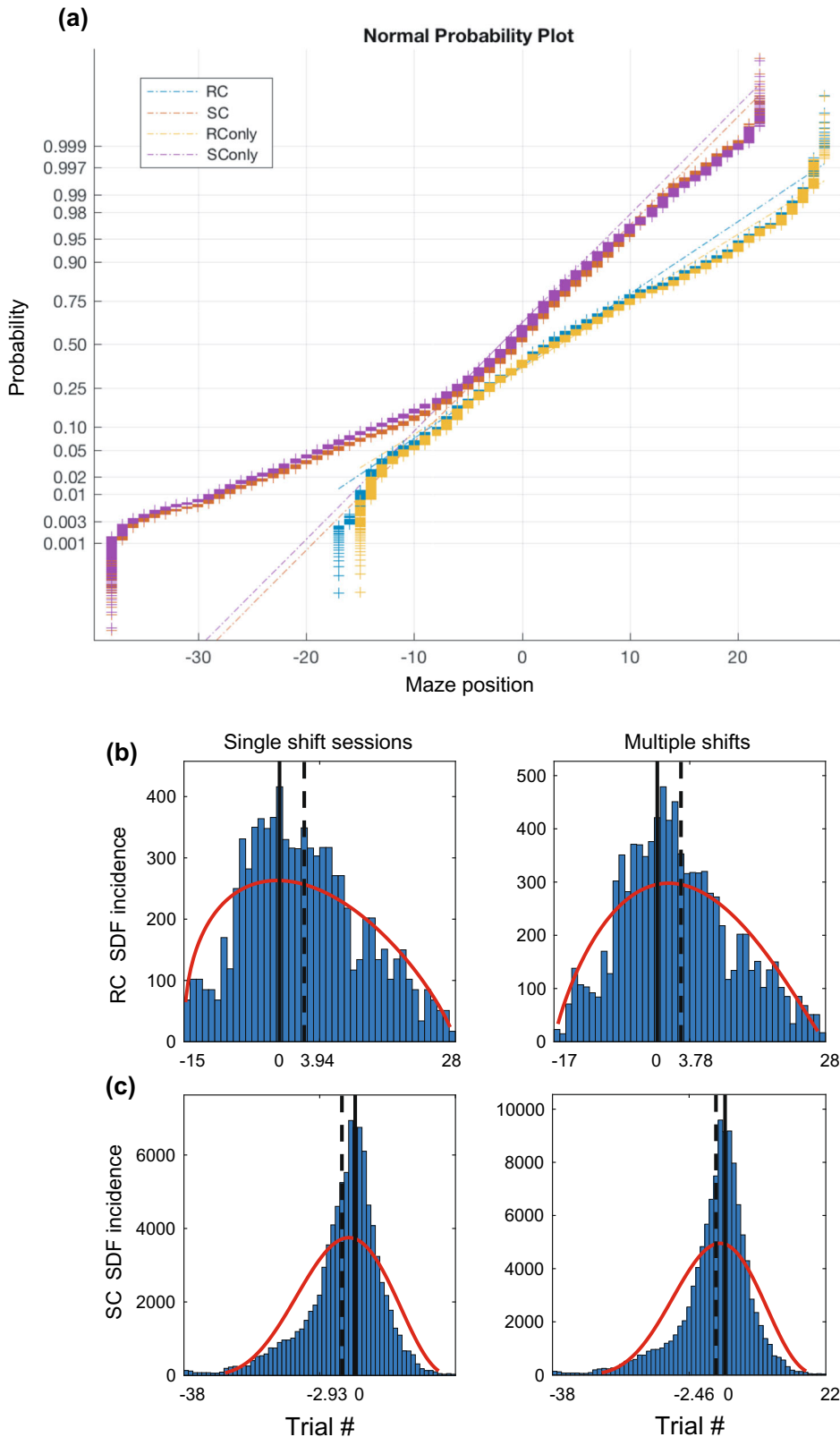


FIGURE 6 Distributions of significant spike density function (SDF) values for rule change (RC)-responsive and strategy change (SC)-responsive neurons. (a) Spatial distributions of significant SDF values do not follow a normal distribution since they deviate from the best fit regression bars (dashed lines). (b,c) Beta distribution fits (red curves) of incidences of significant SDF values for rule and strategy changes, respectively, in either Single shift sessions or Multiple shift sessions. These are analysed separately because multiple behavioural events in the same session could lead to possible confounds. Vertical lines represent the trials when the RC (top row) or SC (bottom row) occurred. Vertical dashed lines represent the means of the fitted beta distribution. The SDF distribution means occur after the RCs but before the SCs.

and thus, this was not a major confound. However, 59 neurons were exclusively correlated with RR. RR correlates have been previously observed in ACC

(e.g., Genovesio et al., 2005) and would be useful for continuous monitoring of task performance levels, complementing the RC responses.

2.5 | Modulation by SWRs and hippocampal theta rhythms

2.5.1 | Modulation of neurons by hippocampal SWRs in RC and SC sessions

Because coordinated HPC and PFC activity during sleep SWRs is implicated in the consolidation of memories (e.g., Girardeau et al., 2009; Maingret et al., 2016; Peyrache et al., 2009; Rothschild et al., 2017), we compared the incidence of neurons reactivated during post-session sleep (S2) after RC as well as SC sessions. The incidence of neurons modulated by SWR in S2 was significantly greater in RC sessions (18.4%) than in Training sessions (8.8%; Figure 7a; $\chi^2 = 9.25$, $df = 1$, $p = .002$). The incidence of SWR modulation in S2 was also greater than S1 in sessions with both an RC and an SC (Figure 7a; $\chi^2 = 7.66$, $df = 1$, $p = .006$). However, the S2 incidence was not significantly above baseline, whereas in S1, it was significantly lower. No significant increase in SWR modulation was observed during any sleep sessions prior to or after an SC session (Figure 7a; χ^2 test, $p > .05$). A significantly higher proportion of all neurons were reactivated during SWRs during S2 than during S1, both in RC-only sessions ($\chi^2 = 5.16$, $df = 1$, $p = .013$; Figure 7a) and in RC + SC sessions ($\chi^2 = 9.12$, $df = 1$, $p = .0014$; Figure 7a). However, this difference was not significant in SC-only sessions ($\chi^2 = 1.41$, $df = 1$, $p = .166$) or in Training sessions ($\chi^2 = 2.22$, $df = 1$, $p = .088$; dashed lines in Figure 7a).

The SWR modulation ratios of neurons reactivated during S1 versus S2 were indistinguishable for RC sessions (1.41 and 1.39, respectively; rank sum test, $p = .85$) and SC sessions (1.60 and 1.41; rank sum test, $p = .085$) or RC + SC sessions (1.42 and 1.39; rank sum test, $p = .81$). In summary, more ACC neurons were modulated by SWR during S2 than in S1 for RC and RC + SC sessions, but not SC sessions, and there was no significant change in the strength of the modulation.

2.5.2 | Hippocampal SWR modulation of cells with identified responses

The next question concerned whether such activity modulations by hippocampal SWRs were specific to neurons with firing rate changes relative to RC or SC or to those with other responses and if, in these particular cases, this modulation was greater in S2 than in S1. Strikingly, a significantly higher proportion of RC-responsive neurons were modulated by ripples during S2 than during S1 ($\chi^2 = 4.23$, $df = 1$, $p = .040$; Figure 7b). This difference

also held in RR responsive neurons ($\chi^2 = 3.85$, $df = 1$, $p = .05$; Figure 7b) and was close to significant in SC-responsive neurons ($\chi^2 = 3.53$, $df = 1$, $p = .06$). In contrast, this was not significant in SV-responsive neurons ($\chi^2 = .634$, $df = 1$, $p = .43$). Importantly, none of the groups had a significantly greater proportion of neurons modulated by SWRs during S1 than unresponsive neurons (χ^2 test, $p > .05$). In S2, the incidences of RC, SC and RR neurons were above baseline ($\chi^2 = 8.4$, 7.1 and 4.4, $df = 1$, $p = .004$, .003 and .04). Thus, the greater proportions of RC- and RR- responsive cells modulated during SWRs in S2 than S1 were not due to sub-baseline values in S1. Among neurons modulated by SWR during both S1 and S2, SC- and RR-responsive neuron proportions were significantly higher than non-responsive neurons ($\chi^2 = 8.3$, $df = 1$, $p = .004$; Figure 7b). This could contribute to maintaining task-relevant information between the two sleep periods.

There were two types of SCs: to rewarded or to unrewarded strategies. The proportions of SWR-modulated neurons in these two groups were not significantly different (S1: 6.7% vs. 3.9%; S2: 4.5% vs. 8.6%, S1 and S2: 5.6% vs. 6.6%, $\chi^2 = 2.99$, $df = 3$, $p = .394$). Similarly, the incidence of SWR modulation in SV-responsive neurons was not significantly different for rewarded versus non-rewarded strategies (S1: 6.0% vs. 2.6%, S2: 8.0% vs. 2.6%, S1 and S2: 1.2% vs. 5.3%; $\chi^2 = 5.20$, $df = 3$, $p = .158$). As observed in computational models of strategy learning (e.g., Dollé et al., 2018), this is consistent with reinforcing values of correct strategies or weakening values of unrewarded strategies each playing symmetrical roles in ACC-dependent learning and would thus be equally reactivated during sleep.

A possible confound is that cells with higher firing rates have a greater chance to be reactivated and modulated by SWRs during sleep (Fernández-Ruiz et al., 2019). Indeed, overall, ripple-modulated neurons here had higher average firing rates (11.9 Hz) during behaviour than non-ripple-modulated neurons (5.6 Hz; Kruskal–Wallis test, $\chi^2 = 155.5$, $df = 1$, $p = .$). However, a two-way ANOVA, with neuron category (SC, RC, SV, RR, non-responsive cells in RC-SC sessions and non-responsive cells in training sessions) and sleep period as factors, revealed no firing rate difference between neurons modulated by ripples in S1 and in S2 ($F = .13$, $df = 1$, $p = .72$), and no significant interaction ($df = 5$, $p = .53$), despite the differences between S1 and S2 reported above. The neuron category factor was significant ($F = 3.3$, $df = 5$, $p = .006$). But the only group with a significantly lower firing rate (RR selective neurons) was the one with a significantly greater incidence of ripple modulation (Tukey–Kramer post hoc test, $p < .05$; Figure S2).

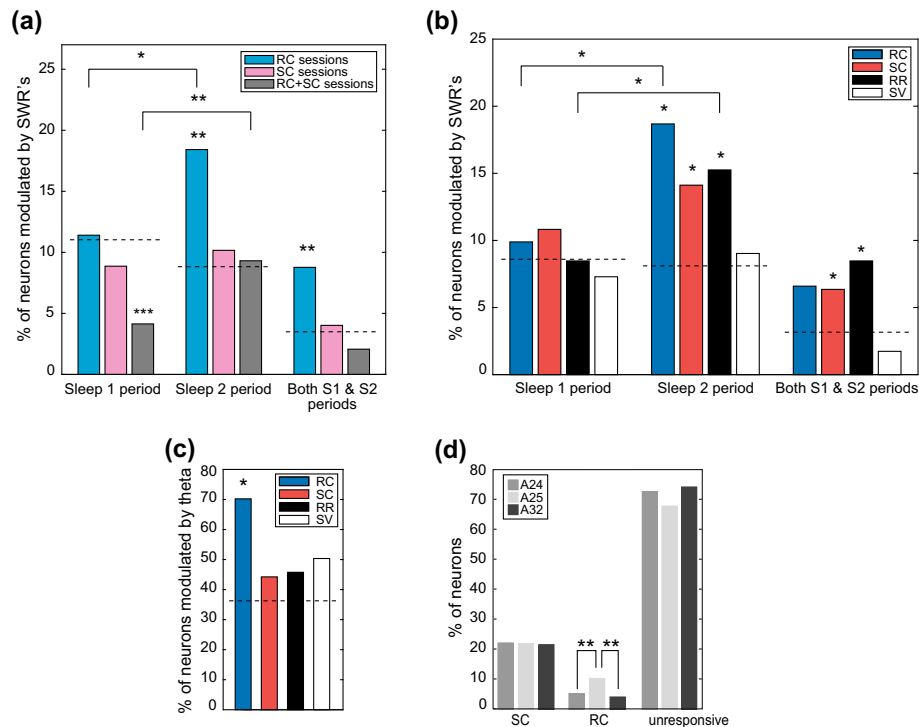


FIGURE 7 Modulation of anterior cingulate cortex (ACC) activity by hippocampal sharp-wave ripples (SWR) and theta oscillations. (a) Incidence of neurons with SWR modulation in sleep before and after sessions with a rule change (RC), a strategy change (SC) and both. Dashed lines indicate reference baseline (here, neurons in Training sessions). ‘Sleep 1 period’ includes neurons modulated by SWR in S1 only, as well as in both S1 and S2. The same holds for ‘Sleep 2 period’. Stars above single bars indicate a significant difference from relative to baseline (dashed line; unresponsive cells recorded in all sessions). (b) Incidence of SWR modulation for SC-, RC-, strategy value and RR responsive cells. Dashed line indicates reference baseline (here, from unresponsive neurons in training sessions). (c) Incidence of theta modulation according to cell response category. Baseline is proportion of unresponsive neurons in all sessions. (d) Anatomical distribution of responses. * $p < .05$; ** $p < .01$; *** $p < .001$.

2.5.3 | Modulation of RC and SC responsive neurons by the hippocampal theta rhythm

During all sessions with a RC and/or a SC, about 39% (838/2127) of the ACC cells analysed were modulated by the HPC theta rhythm (Rayleigh Z tests: $p < .05$). Importantly, HPC theta modulated a significantly greater proportion of RC-selective cells (70%) than unresponsive cells from all sessions, whereas SC-, RR- and SV- neurons did not (Figure 7c). However, there was no significant difference in the modulation strength kappa between RC- and SC-responsive cells (RC: 6.0%, SC: 6.5%; Mann–Whitney test, $z_{val} .096$, rank sum = 3329, $p = .92$; see Figure S2). Differences in incidence of significant theta modulation could not be explained by differences in average firing rates in these groups (Mann–Whitney test, $z_{val} = 1.234$, rank sum = 3692, $p = .22$). (Differences in running speed were not related to differences in incidence of theta modulation; see the [Supporting Information](#)).

2.6 | Anatomical distribution of neurons with activity transitions in relation to RC and SC

The proportion of RC-responsive neurons was higher in A25 than in A24 or A32 (Figure 7d; $\chi^2 = 10.7$, $df = 2$, $p = .0024$). Furthermore, a significantly lower proportion of RC-responsive neurons (7.7%) was located in the dorsal third of A24 (near A32), compared with SC-responsive neurons (21.3%) and unresponsive neurons (19.6%; $\chi^2 = 7.73$, $df = 2$, $p = .0105$). The ratio of pyramidal cells to interneurons did not vary significantly among neurons with the respective response types (74% pyramidal cells for RC-responsive, 80% for SC-responsive, 79% for unresponsive; $\chi^2 = 2.47$, $df = 2$, $p = .15$). Nor did the concentration in superficial versus deep ACC layers vary for RC or SC (38% were in deep layers).

In summary, more ACC neurons were modulated by HPC SWRs during S2 in RC sessions than baseline, and the incidence in S2 was greater than S1 in these sessions

too. Furthermore, modulation by HPC SWRs preferentially occurred in neurons selective for RC, SC and RR, with greater incidence in S2 than S1 for RC and RR. RC-responsive neurons also had a greater incidence of theta modulation than other response types, although all groups had high values. Overall, these results show that modulation by hippocampal theta and SWR was preferentially associated with neurons responsive to changes in task contingencies.

3 | DISCUSSION

Here, populations and substantial proportions of individual ACC neurons responded rapidly after changes in RCs, or in a few trials prior to a SC, and were modulated by SWRs or hippocampal theta rhythms. The experimental design permitted characterization and comparison of the neurons with these two response types in the same data set. In effect, the difficulty of the task permitted comparisons with activity in sessions with no RCs, when the animals spontaneously shifted between different strategies in search for the correct one. Thus, delays between RC and SC were often sufficiently long to permit analyses to distinguish activity changes relative to these respective events, reducing possible confounds. In comparable studies that addressed other questions, RC and SC responses could not always be clearly distinguished (Rich & Shapiro, 2009; Durstewitz et al., 2010; Karlsson et al., 2012; Powell & Redish, 2016; Malagon-Vina et al., 2018; Trouche et al., 2019). Here, we extend upon these and other results by showing that ACC activity also makes abrupt transitions for extradimensional shifts, here between spatial versus sensory discrimination rules and strategies. Trial-by-trial analyses permitted greater precision than trial block analyses. Thus, the population analyses typical of many studies were complemented here by analyses of individual neurons permitting detection of hippocampal theta and SWR modulation.

3.1 | Theta and SWR modulation

Strikingly, a dramatically higher proportion of RC-responsive cells (than SC-, RR-, strategy value-responsive or unresponsive cells) were modulated by hippocampal theta. This is consistent with a theoretical framework wherein the hippocampal theta rhythm coordinates coherent activity in HPC and ACC for registering experiences. This would lead to synaptic modifications underlying labile memory traces through hippocampal neurons firing sequentially in successive phases of theta cycles

(Skaggs et al., 1996; Wagatsuma & Yamaguchi, 2004) and associated PFC activity. SWR events in S2 would correspond to the replay of sequences of hippocampal activity from the preceding behavioural session, and this modulation could correspond to consolidation of memory traces via transmission to the cerebral cortex and ACC in particular (Buzsáki, 1989; review: Girardeau & Zugaro, 2011).

Experimental evidence for this is provided by increased reactivation of neurons during SWR's in S2 compared with S1. During S1, the incidence of hippocampal SWR modulation was indistinguishable among cell groups as well as from baseline values. Furthermore, a significantly higher proportion of in RC- and RR-responsive cells were modulated by SWRs in S2 than S1. This is consistent with a hippocampal contribution to ACC responses to changes in task contingencies, as the HPC responds to mismatches between expectations and observations and novelty (Gray, 1982; Kafkas & Montaldi, 2018; Kumaran & Maguire, 2006; O'Keefe, 1976; Vinogradova, 2001).

The proportion of SWR-modulated SC cells was greater than baseline in S2 but was not significantly greater than S1. Consistent with this, in a study of rats, den Bakker et al. (2023) found that experimental inhibition of the mPFC immediately after hippocampal SWRs impairs responsiveness to changing the rule in a spatial alternation task. The greater incidence of hippocampal SWR modulation of RR-responsive neurons is consistent with the enhanced replay of rewarded trajectories in post-learning sleep (Michon et al., 2019). Interestingly, in an elevated plus maze anxiety paradigm, Adhikari et al. (2011) also found increased ventral hippocampal theta modulation of ACC neurons with task-related responses.

In summary, both theta and SWR modulation could reflect selective transmission of hippocampal system signals that would contribute to these ACC neuronal responses. The high incidence of RC- and RR-responsive neurons suggests a role for HPC-ACC coordination in signalling new environmental contingencies. In SC-responsive neurons, hippocampal signals could contribute to elaborating appropriately adaptive behavioural responses.

Those responsive cells not modulated by sleep SWRs might be expected to be modulated by awake SWRs (Tang et al., 2017). Unfortunately, we did not make reliable recordings of awake SWRs, and thus, we could not test this. Furthermore, because modulation was only investigated in neurons with behavioural correlates during mobility, the present work would not have detected cells active during awake immobility when they would be modulated by SWRs (Yu et al., 2017).

3.2 | ACC neuronal response correlates

The RC- and SC-responsive neurons, as well as the RR- and SV-responsive neurons, could participate in ACC's role in promoting flexible behaviour (Cardinal et al., 2002; Gisquet-Verrier & Delatour, 2006; Granon & Poucet, 2000). ACC lesions impair behavioural flexibility in response to a change in the task rule (de Bruin et al., 1994; Birrell & Brown, 2000; Colacicco et al., 2002; Salazar et al., 2004; Lapis & Morilak, 2006; review: Hamilton & Brigrman, 2015). Moreover, ACC damage particularly impairs performance of tasks requiring shifting from one strategy to another, whether the initial strategy has been learned (Granon & Poucet, 1995; Ragozzino et al., 1999; Ragozzino, Wilcox, et al., 1999) or is spontaneously used by the animal (Granon et al., 1994). Interestingly, here, RC-responsive cells were significantly more concentrated in A25 (formerly, IL) than SC-responsive cells and other unresponsive cells. This is consistent with lesion studies showing that A25 lesions impair visual cue reversal learning, while sparing initial acquisition of visual cue discriminations (Chudasama & Robbins, 2003; Li & Shao, 1998). For goal-directed behaviour (as well as conditioned fear extinction), A25 has been considered to exert a 'stop signal' and also to suppress representations of action-outcome contingencies from influencing behaviour (Barker et al., 2014). Indeed, an optimal response to a RC would require cessation of adherence to the previous rule, consistent with the increased incidence of A25 RC responses here.

Powell and Redish (2016) showed that ACC activity transitions were more related to detecting a task RC and initiating new behavioural strategies than to initiation of the animal's behavioural response per se. Here, we extend these results by showing that the communication between HPC and ACC via theta and SWRs is even greater for the detection of task RCs than for the initiation of new behavioural strategies. Hippocampal contextual information sent to the ACC (and their mutual output structure, the ventral striatum) would be integrated with reward history information to detect task RCs, perhaps in cooperation with the RR-responsive neurons, as well as A24 (Hyman et al., 2017). The rule shifts would be experienced as the failure to consistently receive reward for a previously successful strategy. This is consistent with the concept of the HPC as a detector of mismatch and novelty, as evoked above. Note that the RC-responsive activity occurred on parts of the maze visited prior to the reward site, thus corresponding to contextual rather than simple post-reward responses. Furthermore, RC responses occurred in a population of neurons with no significant activity correlates with RR.

Here, RC and SC associated activity changes in individual neurons were restricted to limited portions of the maze. It is possible that such effects could be masked in population analyses, which average firing over all cells recorded over entire trials. Overall, the population analyses of all neurons showed shifts occurring about 2.5 trials after RC's and about 1 trial before SC's. In contrast, the analyses of individual neurons with behavioural correlates modulated by RC or SC showed averaged responses at about 4 trials after the RC and about 3 trials before the SC's. Because the sampled data sets, calculations and averaging methods are quite different, it is difficult to directly compare the results of the two approaches that suggest that, overall, the population activity responds more rapidly to RC but that individual neuronal activity 'predicts' SCs earlier. Nonetheless, they agree that PFC neurons do anticipate strategy shifts and respond rapidly to RCs.

3.3 | Implications for goal-direction strategy learning

In order to learn and perform goal directed choice tasks, one must learn from recent experience concerning the presence or absence of reward and the association of cues and actions. The durations of the behaviourally correlated ACC activity observed here are suited for this because they could be rather brief or could extend over the order of seconds (cf., Figure 5). Such activity could serve as buffers for working memory and data processing—not only for cues but also for movements, behavioural sequencing and cue-choice contingencies (Procyk & Goldman-Rakic, 2006; Wang & Hayden, 2017). The ACC could be involved in learning associations of concurrent and sequential events including actions (and not just simple cue-action associations) (Del Arco et al., 2017). These processes could lead to development of reward-based strategy learning. The signals recorded here could hence be considered as instrumental for cerebral processing of the stimulus-action-outcome relations that rules represent.

The RC and SC responses could be informed by modality-specific neocortical inputs relevant to the respective strategies (e.g., visual vs. spatial cues for the light–dark vs. left–right tasks, respectively), as well as by thalamic inputs through cortico-striatal loops (Alexander & Crutcher, 1990; Haber, 2003). The changes in activity levels and formation of assemblies of co-activated ACC neurons can be considered to correspond to functionally active modules that would synchronize with and activate subsets of downstream basal ganglia neurons to participate in strategy and behavioural

choices. Such selection among different rules could also be viewed in terms of neural, attentional and behavioural rechanneling. Indeed, other electrophysiological studies have also reported rodent ACC activity to reflect crucial parameters underlying flexible goal-directed behaviours, such as task-related locomotion (Fujisawa et al., 2008; Jung et al., 1998; Poucet, 1997), reward (Miyazaki et al., 2004; Pratt & Mizumori, 2001), working memory (Baeg et al., 2003) and action-outcome contingencies (Kargo et al., 2007; Mulder et al., 2003). Importantly, the RC-responsive and SC-responsive subpopulations in the ACC are relevant to computational studies implicating rat ACC in action selection (e.g., Hasselmo, 2005; Martinet et al., 2011) and in detecting environmental changes (Caluwaerts et al., 2012). Indeed, our results suggest that the rat ACC is well-positioned to combine contingency change detection and strategy selection functions (Holroyd & McClure, 2015), integrating them during behaviour to help build lasting memory traces in conjunction with hippocampal SWRs during sleep.

4 | MATERIALS AND METHODS

4.1 | Rats

Five Long-Evans male adult rats (225–275 g; from the Centre d'Élevage René Janvier, Le Genest-St-Isle, France; [RRID:RGD18337282](https://orcid.org/0000-0001-9145-1000)) were maintained in clear plastic cages bedded with wood shavings. A 12 h/12 h light/dark cycle was applied, and all manipulations took place during the light part of the cycle. The rats were housed in pairs while habituating to the animal facility. They were weighed and handled each workday. Prior to pre-training, they were placed in separate cages, and 14 g of rat chow were provided daily after the pre-training or recording session in order to maintain body weight at not less than 85% of normal values (as calculated for animals of the same age provided ad libitum food and water). The rats were examined daily for their state of health and were fed to satiation at the end of each work week. This level of food deprivation was necessary to motivate performance in the behavioural tasks, and the rats showed neither obvious signs of distress (e.g., excessive or insufficient grooming, hyper- or hypo-activity) nor health problems. The rats were kept in an approved (City of Paris Veterinary Services) animal care facility in accordance with institutional (CNRS Operational Committee for Ethics in the life sciences), national (French Ministère de l'Agriculture, de la Pêche et de l'Alimentation No. 7186) and international (US National Institutes of Health, Helsinki Declaration) guidelines.

4.2 | Surgery

From the start of the pre-training, rats were placed on the mild food deprivation regime. For at least a week before surgery, rats were habituated to running on the Y-maze by allowing them to forage there for 5–25 min daily, with reward available at the end of each arm. Once habituated to the experimental environment (after 7–10 days), rats were anesthetized with intramuscular xylazine (Rompun, .1 ml) and intraperitoneal pentobarbital (35 mg per kg of body weight). Xylocaine solution was injected under the scalp. A drive containing seven tetrodes (six for recording, plus one as reference) was implanted on the skull above the right medial PFC (anterior–posterior, 3.5–5 mm; medial-lateral, .5–1.5 mm). Each tetrode was placed in a 30-gauge stainless steel tube, and the tubes were assembled together in two adjacent rows. Tetrodes were twisted bundles of polyimide coated nichrome wire (13 µm in diameter, Kanthal, Palm Coast, FL). Microdrives allowed independent adjustment of tetrode depth. After retraction of the dura, the rows of cannulae were implanted parallel to the sagittal sinus so that they targeted the superficial and deep layers of the medial bank of the cortex. A separate microdrive containing three tetrodes targeted the ventral HPC (anterior–posterior, –5.0 mm; medial-lateral, 5.0 mm) because the principal projections to ACC originate there (Jay & Whitter, 1991; Thierry et al., 2000). A screw implanted on the occipital bone above the cerebellum served as the reference electrode. The hippocampal tetrodes were lowered to the CA1 pyramidal layer; the depth was adjusted with the help of LFP signs (flat sharp waves, strong ripple oscillations). After surgery, rats recovered for at least 2 weeks while the tetrodes were lowered to reach A24, A32 and A25, as well as the ventral hippocampal CA1 pyramidal layer. Between sessions, tetrodes were gradually lowered to probe different dorso-ventral levels in the ACC.

4.3 | Behavioural task

The Y-maze (Figure 1a) was formed by three arms (85 cm long, 8 cm wide with 2 cm high borders) separated by 120°, with a cylindrical barrier at the centre. The maze area was surrounded by a cylindrical curtain with no explicit cues on it. The rats were habituated to the maze. The rats had to learn by trial-and-error to adapt their behaviour to the current rule in order to maximize the amount of reward received for a given amount of effort. Rats started all trials from the departure arm, and after the central barrier was lowered, a light went on at the end of one of the two goal arms selected in a pseudo-random sequence. The rats then had to select one

of the two choice arms and then go to the end for reward. Chocolate milk rewards (30 μ l) were delivered for choices adhering to the current rule. A photodetector signalled arrivals at the reward trough and triggered a solenoid to release reward when appropriate. On each trial, the reward was available on only one arm. Initially, the animal had to learn that the reward was always located on the right arm, no matter which arm was lit (*Right rule*). Once the animal entered a reward arm, the entrance was blocked, and it was not unblocked until the rat had visited the reward trough (rewarded or not). The rats had been trained to return to the departure arm after the outcome of the trial (rewarded or not), and the barrier was raised until the next trial. To avoid extensive overtraining, a different rule was applied (RC) after the rat had clearly acquired the current rule (i.e., performance reached a criterion level of 10 consecutive rewarded trials) or 11 rewards in the previous 12 trials. This stringent criterion was applied because some rats tended to engage other strategies after initial acquisition, and this assured that the performance had become stable. The RC was not explicitly signalled to the rat in any way and could only be detected by the pattern of unrewarded trials. After acquiring the Right rule, the rat then had to learn to go to the lit arm, regardless of whether it was on the left or on the right (*Light rule*). After that was learned, the rats were successively challenged with a *Left rule* and a *Dark rule* (where the unlit arm was rewarded), and then, in the only rat that succeeded in reaching this level (rat 20), the sequence of task rules was started again from the beginning (*Right, Light, etc.*). All RCs thus qualified as extra-dimensional, engaging spatial or visual cues respectively. No intra-dimensional shifts (reversals) were imposed such as *Right rule* \rightarrow *Left rule* or *Dark rule* \rightarrow *Light rule*, or their inverses, as these have been reported to not require medial PFC function (Birrell & Brown, 2000).

Rats were trained in daily sessions. Each session consisted of 10–60 consecutive trials, stopping when the rat ceased performing. Each session began with the same rule as the final trials of the previous session. Because several sessions were sometimes required to learn certain task rules, there were sessions where no shift in the task rule was imposed. Thus, we will distinguish *shift sessions* (i.e., sessions where a shift in the task rule occurred) from *non-shift sessions*.

4.4 | Data acquisition

Spike waveforms were filtered between 600 and 6000 Hz, digitized with a Power1401 interface (Cambridge Electronic Design, UK) and time-stamped. For this, 32 samples at 32 kHz (1-ms total) were recorded whenever the

signal exceeded a manually set threshold (8 pre-trigger and 24 post-trigger samples). The signal recorded from the same tetrodes was also passed into a low-band filter (between .1 and 475 Hz) in order to extract LFPs. The timestamps of behavioural events (e.g., photodetector crossings) were integrated with the spike data online. A video camera was synchronized with the data acquisition software and monitored the consecutive positions of the animal during the experiment. The video tracking data of the instantaneous position of the animal were acquired using MaxTRAQ[®] (Innovision Systems, Columbiaville, MI) software.

For action potential spike discrimination, the data were processed with a custom Python script for principal component analysis. Then, the Klusters and Klustakwik software (Harris et al., 2000; Hazan et al., 2006; Buzsáki Lab, RRID:SCR_008020) carried out the spike-sorting using the expectation-maximization (EM) algorithm (Celeux & Govaert, 1992). The classifications were then revised manually. Parameters of the EM algorithm were intentionally chosen to extract a high number of clusters (typically from 15 to 60 from the multiple tetrode array). Then those clusters likely to belong to the same unit were merged in manual online analyses.

At the end of experiments, a small electrolytic lesion was made with cathodal current through one wire of each tetrode (25 μ A for 10 s). Rats were euthanized with sodium pentobarbital and perfused with saline then formaldehyde solution (4% v/v). Lesion sites were detected in Nissl stained 60- μ m sections. Positions of recorded neurons were determined with respect to the lesion site by interpolating the measured descent of the electrodes. Electrode sites were reconstructed in three dimensions with the NeuroLucida[®] system.

4.5 | Identification of putative pyramidal cells and interneurons

Putative interneurons and pyramidal cells in ACC were distinguished according to spike width with the method from Barthó et al. (2004). The distribution of spike widths for all ACC neurons was recorded and was bimodal (see fig. S6 in Benchenane et al., 2010). Cells with spike widths inferior to .3 ms were classified as putative interneurons, whereas those superior to .35 ms were considered as putative pyramidal cells.

4.6 | Behavioural analyses

Each trial was characterized by parameters including the current task rule (right, light, left or dark), the position of

the light (right or left), the arm chosen by the animal (right or left) and the outcome of the trial (rewarded or not).

Two principal events were the bases for the analyses of behavioural and neurophysiological data from each trial: *Start* and *Arrival*. The trial Start time was extracted from the video tracked position data and was defined as the onset of initial forward acceleration in the departure arm. The Arrival event was defined as the instant when the animal first blocked the photodetector at the reward reservoir of the selected arm.

Next, to systematically categorize the animal's behaviour in terms of the 'strategy' it followed, the behavioural data from all of the sessions were concatenated for each animal. A custom script scanned these files and extracted series of trials where the animal's behavioural strategy was consistently stable ('blocks of trials'). The strategies considered in the behavioural analyses included: (1) Going to the right arm regardless of the visual cue ('Right' strategy); (2) 'Left'; (3) Going to the lit arm, regardless of whether it was to the right or left ('Light' strategy); (4) 'Dark'; and (5) Spatial 'Alternation' (not rewarded) (see Figure 1a). Trials not included in such blocks are considered as a sixth 'Undefined' strategy, whereas the five are termed 'Defined'. We systematically searched for higher order strategies (e.g., left-left-right-right-left-left) but found insufficient evidence for them. Note also that a single trial could be compliant with two strategies (for instance Left and Dark) or even three strategies (for instance Left, Dark and Alternation), but the randomization of the light positions assured that blocks of 4 or more trials could not comply with more than one strategy.

To determine the minimum number of strictly compliant trials to be considered a strategy block, we performed simulations consisting of 1.6×10^7 random runs. Each of these runs included the 3322 trials of the data set, with the same sequence of rules and lit arm positions, but the arm choices were randomly generated. These simulations showed that for blocks of length 6 or greater, the only 5.4% of random arm choices would belong to such a block for each single strategy. Thus, 95% of random moves would not belong to such a block. Hence, we considered a block to be strictly compliant to one of the five Defined strategies if it contained a continuous sequence of at least 6 trials such that all the rat's choices were compliant with that strategy. This is the same or even more stringent criterion than used in this type of study (e.g., Kaefer et al., 2020; Lapid-Bluhm et al., 2009; Tait et al., 2017).

Because rats occasionally made non-compliant (NC) choices within long runs of compliant trials, we also considered as strategy blocks those sequences containing

at least 9 trials with only one NC trial. For example, if the animal's choices were compliant (C) with a strategy for 6 trials, NC for 1 trial and then C again for 2 trials, the whole block of 9 trials is considered as a 'leniently compliant' strategy block. Following the same principle, we included blocks of CCCC-NC-CCC (and its reverse) or CCCC-NC-CCCC. Longer sequences might include several NC trials providing that these rules were respected. In simulations as described above, the probability that a random choice would belong to a leniently compliant block for each of the strategies was only 8.6%; 91.4% of random moves would not belong to such a block.

To gauge the risk that sequences detected with these criteria could have occurred stochastically, the incidence of leniently compliant sequences was computed in simulations of 1.6×10^7 random runs. Each random run included the 3322 trials of the data set, with the same sequence of rules and lit arm positions, but the arm choices were randomly generated. These simulations yielded values of the mean, median and 95% confidence intervals for the percentages of trials that would have stochastically appeared in leniently compliant blocks of length greater than or equal to 6 trials (Table 1 and Annex in Supporting Information). For all of the strategies, the incidence of experimental trials in blocks compliant to the respective strategies is outside of the confidence interval limits, inconsistent with fortuitous compliance by means of stochastic choices. Similarly, the incidence of trials following any defined strategy (78.2%) greatly exceeded the confidence interval upper bound (43.7%).

To verify that the results of these analyses were not dominated by very long sequences that were clearly not stochastic, we further examined smaller blocks of 11 trials or less (which composed 99.1% of the trials in randomly generated choices). Over these respective block lengths, 40% of the actual values fell outside the $p < .05$ confidence limits, again providing evidence against stochastic choices.

The performance of the animals prior to initial rule acquisition was also inconsistent with stochastic behaviour. Four of the five animals reached criterion for the R rule in the very first training session (cf., values in Results 'Behaviour'), corresponding to fewer trials than expected by chance. During the initial acquisitions, the incidence of occurrence of sequences compliant with a rule currently not being rewarded also extended beyond the lower or upper bounds of the confidence intervals of the randomized data simulation.

SCs are defined as two consecutive blocks where the rat followed different strategies (e.g., the animal performs a series of 10 trials following the *Light* strategy, always

TABLE 1 Incidences of trials in leniently compliant blocks of length >5 . At left are results for the simulations described in the text. Actual values are from animal data. Note that blocks compliant with different specific strategies could partially overlap, so that the sum of trials for the five strategies does not equal that of defined trials.

Strategy	Simulation results (% trials in blocks)				Actual values	
	Mean	Median	Lower bound (2.5%)	Upper bound (97.5%)	%	<i>n</i>
Left	8.6	8.6	5.8	11.6	27.0	896
Right	8.6	8.6	5.8	11.6	22.0	730
Light	8.6	8.6	5.8	11.6	23.4	776
Dark	8.6	8.6	5.8	11.6	6.9	229
Alternation	8.6	8.6	5.8	11.6	13.8	459
Defined	38.9	38.9	34.2	43.7	78.2	2599
Undefined	61.1	61.1	56.3	65.8	21.8	723

going to the lit arm, and then performs a series of 6 trials following the *Alternation* strategy). We define *extradi-mensional shifts* as SC between spatial and visual strategies (or vice versa), such as Left then Dark strategy.

4.7 | Experimental design and statistical analyses

Neuronal activity was recorded as the rats performed in a completely automated maze or during sleep immediately preceding and following this. Each neuron served as its own control, and activity levels were compared before versus after events with analyses and statistical tests as described in the following sections. The tests include bootstrap Monte Carlo analyses, ANOVA, *t* tests, Kruskal–Wallis, Mann–Whitney, χ^2 and Rayleigh *Z* tests. The specific applications of these tests are explained below and in Section 2 (insufficient sampling precluded analyses of rapid eye movement [REM] sleep).

4.8 | Activity transition analyses at the population level

An unbiased automatic decomposition of the trials in each session into blocks determined whether the onsets of transitions in neural activity are most closely temporally associated to behavioural (SC) or task (RC) changes. Similar to Powell and Redish (2016), for each trial in a given session, we computed a population vector from the firing rate of each given neuron averaged over the entire trial (from *Start* until *Arrival*) from all ACC cells recorded simultaneously. Each population vector was *z*-scored in order to give the same weight to cells with low and high firing rates. We then computed the correlation

matrix where each element E_{ij} is the correlation between population vectors of trials *i* and *j* for all trials of the session.

When displayed graphically, blocks of high values in the correlation matrix indicate series of trials with correlated population activity. We performed an automated search for such blocks by detecting the best decomposition of the matrix into blocks, that is, finding the optimal partition of blocks of trials along the diagonal of the matrix, so that eliminating elements outside the blocks minimizes the amount of information lost. Information loss was measured as the percentage by which the sum of absolute values of the elements in the matrix is reduced after exclusion of the elements outside the blocks. To prevent the trivial decomposition (i.e., a single block encompassing everything) from being systematically considered as the one that minimizes the loss (as it has no loss of information), we rejected it if at least one decomposition into 2 or more blocks led to a loss of less than 1/3 of the information (i.e., if the information present within the blocks was superior or equal to 2/3 of total information within the matrix). Otherwise, no decomposition was retained, which was interpreted as no substantial change in population activity having occurred during that session.

In order to find the best decomposition into two or more blocks, we tested all possible decompositions of each matrix into blocks (with each block including at least 3 trials and at most 2/3 of the trials of the session). Then for each decomposition, we projected the original matrix onto the considered blocks (which are concentrated around the diagonal of the matrix), hence setting to zero the elements outside the blocks. This tests the hypothesis that the correlations of activity between blocks are negligible, as if the population activity has sharp state changes between blocks of trials. Then, for

TABLE 2 Session ID numbers, animal identifiers and numbers of neurons in population analyses of Figure 3.

ID number	Rat #	# neurons
1	5	26
2	2	21
3	3	57
4	3	46
5	1	NA
6	5	19
7	5	21
8	5	15
9	5	23
10	5	19
11	5	13
12	5	28
13	5	23
14	5	21
15	2	8
16	2	19
17	2	NA
18	2	NA
19	5	14
20	3	37
21	5	14
22	2	13
23	3	52
24	2	NA
25	3	44
26	3	52
27	5	21
28	5	19
29	2	31
30	4	25
31	4	NA
32	5	21
33	5	50
34	5	22
35	5	13
36	5	19
37	5	21
38	2	18
39	5	22
40	2	24
41	3	56

each decomposition, we measured how much information was lost and retained the one that minimized this amount.

We developed this approach to decompose the population cross-correlation matrix rather than use k-means clustering employed by Powell and Redish (2016) because it was not clear that the data satisfied the requirements of k-means. Firstly, k-means is based on the principle of spherical clusters that can be separated in such a manner that the means approach the centres of the respective clusters. Furthermore, the clusters should have comparable sizes. But, here, we expected sharp transitions between series of trials with respectively homogeneous firing rates, and the transitions could occur early or late in the session, creating groups of unequal size. Furthermore, it was not clear how many clusters to preset in the k-means algorithm because RC and SC could each occur one or more times in the same session, and the recorded populations only had limited numbers of neurons, leading some of these to not respond to some RCs or SCs. There was also concern that the algorithm would stop at local minima, rather than at more optimal solutions.

4.8.1 | Estimating timing of population activity transitions relative to RC or SC events

In order to quantify the possible relationship between an activity transition detected on a particular trial i with a RC or SC event occurring on trial j , the difference between i and j was taken if there was only one such event. If there were two or more events of the same or different types (i.e., RC or SC), the one occurring the fewer number of trials from the activity transition was selected. Possible ambiguities could occur when an RC was rapidly followed by an SC. Thus, analyses were first performed only on sessions where only one such event occurred. Activity changes associated with RC were only considered for the first trial after a conflict between the RC and the previous rule was detectable (as individual behavioural choices could be consistent with more than one rule).

4.9 | Event-locked analyses for activity transitions in single neurons

Activity in time windows bracketing salient trial events were compared in trials prior to and after RC and SC. The four periods included *pre-start*, in the time window [$Start - 2.5$ s; $Start$]; *post-start* [$Start$; $Start + 2.5$ s];

pre-arrival [*Arrival* - 2.5 s; *Arrival*]; and *post-arrival* [*Arrival*; *Arrival* + 1.25 s]. The post-arrival period was restricted to 1.25 s in order to restrict to the period when the rats were immobile irrespective of whether the trial was rewarded or not. This avoided possible confounds with different motor behaviours in rewarded and non-rewarded trials. In 96.4% of all trials recorded in the five animals (including rewarded and unrewarded trials), the rats remained at the reward site for at least 1.25 s.

The Wilcoxon-Mann-Whitney test examined differences in neuronal firing rate around RC and SC events. This was tested for each of the four trial event windows (with Bonferroni corrections for multiple comparisons).

To confirm and expand upon these analyses, a bootstrap Monte Carlo analysis was also performed for each cell, again with separate tests for each of the four periods. In all cases, the firing rates were compared between trial blocks before and after the RC or SC. Then the activity of these trials was randomly re-attributed to two surrogate sets with the same numbers of trials, and the difference was taken. This shuffling procedure was repeated 5000 times and yielded a distribution from which only those differences in firing rate with *p* values falling within the upper or lower 2.5% of the shuffled distributions were considered as significant transitions in neural activity. To quantify the incidence of spontaneous changes of firing rate of PFC neurons in sessions where the rat consistently performed a single strategy, the first half of the session was compared with the second half with the same bootstrap Monte Carlo analysis. Because the latter tests (reported in Section 2) showed that a non-negligible number of significant transitions in firing rate occurred in the sessions with no SCs or RCs (or other apparent behavioural differences), further complementary analyses were performed.

4.10 | Estimating timing of individual neuron activity transitions relative to RC or SC events

The preceding analysis groups data from different maze positions. It presumes that activity shifts will only take place at RCs or SCs. Another analysis without this a priori assumption examined each neuron's activity to determine on which trial (if any) there was the maximal significant difference between firing rates in the block of trials before and after that trial. The nonparametric analysis developed by Fujisawa et al. (2008) constructs bootstrap confidence intervals of positional SDFs. The null hypothesis posits no difference in firing between trials before and after the event of interest (here, RC and SC). Sessions were divided into all possible pairs of sets of contiguous trials, with a minimum of four trials in each set.

Thus, if a session had 50 trials, trials 1–4 were compared with 5–50, 1–5 versus 6–50, 1–6 versus 7–50, [...], through trials 1–46 versus 47–50. SDFs were determined for each of the pairs of sets of trials.

Here, data could only be analysed for positions that the rat occupied on every trial of the session, and other data (particularly on the start arm, where the rats did not always go to the end) were excluded. Data were divided into spatial bins of length 1.75 cm along the linearized trajectory from starting point to reward site (each corresponding to 2.5 pixels in the video image; *x*-axis of 1st and 2nd columns of Figure 5).

For each pair of trial blocks, a bootstrap Monte Carlo analysis randomly redistributed all of the trials in the session to surrogate pairs of sets with the same respective numbers of trials as the original sets. For each surrogate set, a spike rate function across the spatial bins was taken as a set of points on the maze where the spikes occurred, and this was transformed to a spike count function with a Gaussian kernel whose bandwidth is 2 bins (=3.5 cm). Dividing the spike count functions by the time spent in each position over all of the trials for the respective parts of the session yielded the spike rate functions. The pre-versus post-transition difference was then computed for each block of trials.

To determine the statistical significance of these rate differences, the distribution of the rate difference statistics was estimated by randomly reassigning the data from each trial into two surrogate groups 5000 times. For each of the spatial bins, a pointwise confidence band with a *p* value of .05 was assigned to the 125 greatest positive and negative differences respectively (a two-way test). Because the pointwise confidence band is computed at multiple points, the confidence level must be corrected for these multiple comparisons. This is achieved by computing the global confidence band: first, we calculate the 'global confidence level', taken as the percentage of resampled rate differences whose values are not all inside the area limited by the pointwise band. The procedure is repeated to build the pointwise confidence band by gradually decreasing the value of the pointwise confidence limit until the global limit is equal to .05. Then, a maze zone is considered to have significant difference in pre- versus post-transition firing only if this difference crosses both the global and pointwise bands, but the extent of this zone is determined only by the points where it lies beyond the pointwise band (Fujisawa et al., 2008; also see Catanese et al., 2012).

To control for possible spatial selectivity in the ACC responses (Euston et al., 2007), analyses were repeated separately using only data from either left or right choice trials in sessions where sample sizes were large enough (see also Lindsay et al., 2018). This showed that 43 (73%; or 34% of the total of 127 neurons) retained significant SDF

differences when either left or right choice trials were analysed alone, and thus, their transition related activity changes are not confounded with location-selective firing.

4.10.1 | Multiple regression analysis of single-unit activity with strategy value and RR

In order to control for potential confounds in putative RC- and SC-responses, we constructed several regressors and then tested for correlation with single cell activity with a multiple regression analysis.

We first built a simple and parsimonious (without any free parameters) regressor mimicking progressively learned strategy values in computational models (Dollé et al., 2018). This consisted of the estimated value of the three observed strategies: V_{Right} , V_{Light} and $V_{\text{Alternation}}$ (V_{Left} being equal to $-V_{\text{Right}}$ and $V_{\text{Dark}} = -V_{\text{Light}}$). These values were initialized at 0 at the beginning of each new session. After each trial, the value of a strategy X was increased by 1 if the animal's behaviour was consistent with it and got rewarded, decreased by 1 if it was inconsistent and got rewarded. Furthermore, the value was decreased by 1 if it was consistent but unrewarded and increased by 1 if it was both inconsistent and unrewarded. For example, if at trial N , the animal went to the left arm which was lit, and received a reward, then V_{Light} was increased by 1 while V_{Right} was decreased by 1.

We then built a second regressor representing the RR and computed over a 6-trial sliding window. We finally also included regressors representing the lit arm on the current trial (L ; 0 for left or for 1 right), arm choice (C ; 0 for left or 1 for right) and reward (R ; 0 or 1).

The spike rate $y(t)$ in trial t was then analysed using the following multiple linear regression model:

$$y(t) = \rho_0 + \rho_1 V_{\text{Right}}(t) + \rho_2 V_{\text{Light}}(t) + \rho_3 V_{\text{Alternation}}(t) + \rho_4 RR(t) + \rho_5 L(t) + \rho_6 C(t) + \rho_7 R(t),$$

where ρ_i ($i \in \{1..7\}$) are the regression coefficients.

Following Seo and Lee (2009) and Khamassi et al. (2015), we applied a restrictive significance threshold permitting only 5% significance after permuting the trial order 10,000 times (bootstrap method) so that this regression model would not suffer from violation of independence between regressors.

4.11 | LFP analyses

Each of the mid-ventral hippocampal tetrodes was electrically connected in a single-electrode configuration (all channels shorted together) and used for LFP recordings.

The screw implanted in the occipital bone above the cerebellum was the reference. LFPs were sampled and stored at 2 kHz. Theta was filtered at 5–10 Hz. Theta modulation of cell activity was detected with the Rayleigh test with a criterion of $p < .05$. Detecting SWRs and measuring SWR modulation of cell activity employed the methods of Peyrache et al. (2009). For the latter, PETH's plotted cell activity relative to ripples with 100-ms bins. A t test compared the central bin with the baseline value.

For information about and access to the recording database, see <https://ccrns.org/data-sets/pfc/pfc-6/about-pfc-6>.

AUTHOR CONTRIBUTIONS

M. Khamassi: Conceptualization; data curation; formal analysis; investigation; methodology; software; visualization; writing — original draft; writing — review and editing. **A. Peyrache:** Data curation; formal analysis; funding acquisition; software. **K. Benchenane:** Formal analysis. **David Hopkins:** Investigation; methodology; visualization. **N. Lebas:** Formal analysis; software. **V. Douchamps:** Investigation; writing — review and editing. **J. Droulez:** Formal analysis; funding acquisition; software; writing — original draft; writing — review and editing. **F. P. Battaglia:** Conceptualization; formal analysis; investigation; methodology; project administration; supervision; validation; writing — review and editing. **S. I. Wiener:** Conceptualization; funding acquisition; methodology; project administration; supervision; writing — original draft; writing — review and editing.

ACKNOWLEDGEMENTS

We thank Prof. J.-M. Deniau, Drs. A.-M. Thierry, Y. Gioanni, M.B. Zugaro, R. Todorova and E. Cerasti for valuable discussions, S. Doutrémer for histology, F. Maloumian for help with figures, N. Quenech'du for help with the 3-D anatomical reconstructions, Y. Dupraz for mechanical engineering and Prof. A. Berthoz for support throughout the project.

CONFLICT OF INTEREST STATEMENT

None of the authors have any financial or non-financial competing interests.

PEER REVIEW

The peer review history for this article is available at <https://www.webofscience.com/api/gateway/wos/peer-review/10.1111/ejn.16496>.

DATA AVAILABILITY STATEMENT

The electrophysiological data are available at Adrien Peyrache, Mehdi Khamassi, Karim Benchenane, Sidney I Wiener, Francesco Battaglia (2018); Activity of neurons

in rat medial prefrontal cortex during learning and sleep. *CRCNS.org* <https://doi.org/10.6080/K0KH0KH5>.

ORCID

M. Khamassi  <https://orcid.org/0000-0002-2515-1046>

V. Douchamps  <https://orcid.org/0000-0002-2795-861X>

S. I. Wiener  <https://orcid.org/0000-0002-5819-1319>

REFERENCES

- Adhikari, A., Topiwala, M. A., & Gordon, J. A. (2011). Single units in the medial prefrontal cortex with anxiety-related firing patterns are preferentially influenced by ventral hippocampal activity. *Neuron*, *71*(5), 898–910. <https://doi.org/10.1016/j.neuron.2011.07.027>
- Alexander, G. E., & Crutcher, M. D. (1990). Functional architecture of basal ganglia circuits: Neural substrates of parallel processing. *Tins*, *13*(7), 266–271.
- Arikuni, T., Sako, H., & Murata, A. (1994). Ipsilateral connections of the anterior cingulate cortex with the frontal and medial temporal cortices in the macaque monkey. *Neuroscience Research*, *21*(1), 19–39. [https://doi.org/10.1016/0168-0102\(94\)90065-5](https://doi.org/10.1016/0168-0102(94)90065-5)
- Baeg, E. H., Kim, Y. B., Huh, K., Mook-Jung, I., Kim, H. T., & Jung, M. W. (2003). Dynamics of population code for working memory in the prefrontal cortex. *Neuron*, *40*(1), 177–188. [https://doi.org/10.1016/S0896-6273\(03\)00597-X](https://doi.org/10.1016/S0896-6273(03)00597-X)
- Barker, J. M., Taylor, J. R., & Chandler, L. J. (2014). A unifying model of the role of the infralimbic cortex in extinction and habits. *Learning & Memory*, *21*(9), 441–448. <https://doi.org/10.1101/lm.035501.114>
- Barthó, P., Hirase, H., Monconduit, L., Zugaro, M. B., Harris, K. D., & Buzsáki, G. (2004). Characterization of neocortical principal cells and interneurons by network interactions and extracellular features. *Journal of Neurophysiology*, *92*, 600–608. <https://doi.org/10.1152/jn.01170.2003>
- Benchenane, K., Peyrache, A., Khamassi, M., Tierney, P., Gioanni, Y., Battaglia, F. P., & Wiener, S. I. (2010). Coherent theta oscillations and reorganization of spike timing in the hippocampal-prefrontal network upon learning. *Neuron*, *66*(6), 921–936. <https://doi.org/10.1016/j.neuron.2010.05.013>
- Berg, E. A. (1948). A simple objective test for measuring flexibility in thinking. *The Journal of General Psychology*, *39*, 15–22. <https://doi.org/10.1080/00221309.1948.9918159>
- Birrell, J. M., & Brown, V. J. (2000). Medial frontal cortex mediates perceptual attentional set shifting in the rat. *The Journal of Neuroscience*, *20*(11), 4320–4324. <https://doi.org/10.1523/JNEUROSCI.20-11-04320.2000>
- Bissonette, G. B., Powell, E. M., & Roesch, M. R. (2013). Neural structures underlying set-shifting: Roles of medial prefrontal cortex and anterior cingulate cortex. *Behavioural Brain Research*, *250*, 91–101. <https://doi.org/10.1016/j.bbr.2013.04.037>
- Bunge, S. A. (2004). How we use rules to select actions: A review of evidence from cognitive neuroscience. *Cognitive, Affective, & Behavioral Neuroscience*, *4*(4), 564–579. <https://doi.org/10.3758/CABN.4.4.564>
- Buzsáki, G. (1989). Two-stage model of memory trace formation: A role for “noisy” brain states. *Neuroscience*, *31*(3), 551–570. [https://doi.org/10.1016/0306-4522\(89\)90423-5](https://doi.org/10.1016/0306-4522(89)90423-5)
- Caluwaerts, K., Staffa, M., N’Guyen, S., Grand, C., Dollé, L., Favre-Félix, A., Girard, B., & Khamassi, M. (2012). A biologically inspired meta-control navigation system for the Psikharpax rat robot. *Bioinspiration & Biomimetics*, *7*(2), 025009. <https://doi.org/10.1088/1748-3182/7/2/025009>
- Cardinal, R. N., Parkinson, J. A., Hall, J., & Everitt, B. J. (2002). Emotion and motivation: The role of the amygdala, ventral striatum and prefrontal cortex. *Neuroscience and Biobehavioral Reviews*, *26*(3), 321–352. [https://doi.org/10.1016/S0149-7634\(02\)00007-6](https://doi.org/10.1016/S0149-7634(02)00007-6)
- Catanese, J., Cerasti, E., Zugaro, M. B., Viggiano, A., & Wiener, S. I. (2012). Dynamics of decision-related activity in hippocampus. *Hippocampus*, *22*(9), 1901–1911. <https://doi.org/10.1002/hipo.22025>
- Celeux, G., & Govaert, G. (1992). A classification EM algorithm for clustering and two stochastic versions. *Computational Statistics and Data Analysis*, *14*(3), 315–332. [https://doi.org/10.1016/0167-9473\(92\)90042-E](https://doi.org/10.1016/0167-9473(92)90042-E)
- Chiang, F.-K., Wallis, J. D., & Rich, E. L. (2022). Cognitive strategies shift information from single neurons to populations in prefrontal cortex. *Neuron*, *110*(4), 709–721. <https://doi.org/10.1016/j.neuron.2021.11.021>
- Chudasama, Y., & Robbins, T. W. (2003). Dissociable contributions of the orbitofrontal and infralimbic cortex to Pavlovian auto-shaping and discrimination reversal learning: Further evidence for the functional heterogeneity of the rodent frontal cortex. *The Journal of Neuroscience*, *23*, 8771–8780. <https://doi.org/10.1523/JNEUROSCI.23-25-08771.2003>
- Colacicco, G., Welzl, H., Lipp, H., & Würbel, H. (2002). Attentional set-shifting in mice: Modification of a rat paradigm, and evidence for strain-dependent variation. *Behavioural Brain Research*, *132*, 95–102. [https://doi.org/10.1016/S0166-4328\(01\)00391-6](https://doi.org/10.1016/S0166-4328(01)00391-6)
- de Bruin, J. P. C., Sánchez-Santed, F., Heinsbroek, R. P., Donker, A., & Postmes, P. (1994). A behavioural analysis of rats with damage to the medial prefrontal cortex using Morris water-maze: Evidence for behavioural flexibility, but not for impaired spatial navigation. *Brain Research*, *652*, 323–333. [https://doi.org/10.1016/0006-8993\(94\)90243-7](https://doi.org/10.1016/0006-8993(94)90243-7)
- del Arco, A., Park, J., Wood, J., Kim, Y., & Moghaddam, B. (2017). Adaptive encoding of outcome prediction by prefrontal cortex ensembles supports behavioral flexibility. *The Journal of Neuroscience*, *37*(35), 8363–8373. <https://doi.org/10.1523/JNEUROSCI.0450-17.2017>
- den Bakker, H., van Dijck, M., Sun, J. J., & Kloosterman, F. (2023). Sharp-wave-ripple-associated activity in the medial prefrontal cortex supports spatial rule switching. *Cell Reports*, *42*(8), 112959. <https://doi.org/10.1016/j.celrep.2023.112959>
- D’Esposito, M., Detre, J. A., Alsop, D. C., Shin, R. K., Atlas, S., & Grossman, M. (1995). The neural basis of the central executive system of working memory. *Nature*, *378*(6554), 279–281. <https://doi.org/10.1038/378279a0>
- Dias, R., Robbins, T. W., & Roberts, A. C. (1996). Dissociation in prefrontal cortex of affective and attentional shifts. *Nature*, *380*(6569), 69–72. <https://doi.org/10.1038/380069a0>
- Dollé, L., Chavarriaga, R., Guillot, A., & Khamassi, M. (2018). Interactions between spatial strategies producing generalization gradient and blocking: A computational approach. *PLoS Computational Biology*, *14*(4), e1006092. <https://doi.org/10.1371/journal.pcbi.1006092>

- Drewe, E. A. (1974). The effect of type and area of brain lesion on Wisconsin card sorting test performance. *Cortex*, *10*, 159–170. [https://doi.org/10.1016/S0010-9452\(74\)80006-7](https://doi.org/10.1016/S0010-9452(74)80006-7)
- Durstewitz, D., Vittoz, N. M., Floresco, S. B., & Seamans, J. K. (2010). Abrupt transitions between prefrontal neural ensemble states accompany behavioral transitions during rule learning. *Neuron*, *66*, 438–448. <https://doi.org/10.1016/j.neuron.2010.03.029>
- Eschenko, O., Ramadan, W., Mölle, M., Born, J., & Sara, S. J. (2008). Sustained increase in hippocampal sharp-wave ripple activity during slow-wave sleep after learning. *Learning & Memory*, *15*(4), 222–228. <https://doi.org/10.1101/lm.726008>
- Euston, D. R., Tatsuno, M., & McNaughton, B. L. (2007). Fast-forward playback of recent memory sequences in prefrontal cortex during sleep. *Science*, *318*(5853), 1147–1150. <https://doi.org/10.1126/science.1148979>
- Fernández-Ruiz, A., Oliva, A., Fermino de Oliveira, E., Rocha-Almeida, F., Tingley, D., & Buzsáki, G. (2019). Long-duration hippocampal sharp wave ripples improve memory. *Science*, *364*(6445), 1082–1086. <https://doi.org/10.1126/science.aax0758>
- Frankland, P. W., & Bontempi, B. (2005). The organization of recent and remote memories. *Nature Reviews Neuroscience*, *6*(2), 119–130. <https://doi.org/10.1038/nrn1607>
- Fries, P. (2015). Rhythms for cognition: Communication through coherence. *Neuron*, *88*(1), 220–235. <https://doi.org/10.1016/j.neuron.2015.09.034>
- Fujisawa, S., Amarasingham, A., Harrison, M. T., & Buzsáki, G. (2008). Behavior-dependent short-term assembly dynamics in the medial prefrontal cortex. *Nature Neuroscience*, *11*, 823–833.
- Gallistel, C. R., Fairhurst, S., & Balsam, P. (2004). The learning curve: Implications of a quantitative analysis. *PNAS*, *101*, 13124–13131. <https://doi.org/10.1073/pnas.0404965101>
- Genovesio, A., Brasted, P. J., Mitz, A. R., & Wise, S. P. (2005). Prefrontal cortex activity related to abstract response strategies. *Neuron*, *47*, 307–320. <https://doi.org/10.1016/j.neuron.2005.06.006>
- Girardeau, G., Benchenane, K., Wiener, S. I., & Buzsáki, Z. M. B. (2009). Selective suppression of hippocampal ripples impairs spatial memory. *Nature Neuroscience*, *12*(10), 1222–1223. <https://doi.org/10.1038/nn.2384>
- Girardeau, G., & Zugaro, M. (2011). Hippocampal ripples and memory consolidation. *Current Opinion in Neurobiology*, *21*(3), 452–459. <https://doi.org/10.1016/j.conb.2011.02.005>
- Gisquet-Verrier, P., & Delatour, B. (2006). The role of the rat prelimbic/infralimbic cortex in working memory: Not involved in the short-term maintenance but in monitoring and processing functions. *Neuroscience*, *141*(2), 585–596. <https://doi.org/10.1016/j.neuroscience.2006.04.009>
- Goldman-Rakic, P. S. (1987). Circuitry of primate prefrontal cortex and regulation of behavior by representational memory. In F. Plum (Ed.), *Higher functions of the brain: The nervous system; handbook of physiology* (Vol. V) (pp. 373–417). American Physiological Society. <https://doi.org/10.1002/cphy.cp010509>
- Goldman-Rakic, P. S. (1995). Cellular basis of working memory. *Neuron*, *14*(3), 477–485. [https://doi.org/10.1016/0896-6273\(95\)90304-6](https://doi.org/10.1016/0896-6273(95)90304-6)
- Granon, S., & Poucet, B. (1995). Medial prefrontal lesions in the rat and spatial navigation: Evidence for impaired planning. *Behavioral Neuroscience*, *109*(3), 474–484. <https://doi.org/10.1037/0735-7044.109.3.474>
- Granon, S., & Poucet, B. (2000). Involvement of the rat prefrontal cortex in cognitive functions: A central role for the prelimbic area. *Psychobiology*, *28*(2), 229–237. <https://doi.org/10.3758/BF03331981>
- Granon, S., Vidal, C., Thinus-Blanc, C., Changeux, J. P., & Poucet, B. (1994). Working memory, response selection, and effortful processing in rats with medial prefrontal lesions. *Behavioral Neuroscience*, *108*(5), 883–891. <https://doi.org/10.1037/0735-7044.108.5.883>
- Grant, D. A., Jones, O. R., & Tallant, B. (1949). The relative difficulty of the number, and color concepts of a Weigle-type problem. *Journal of Experimental Psychology*, *39*, 552–557. <https://doi.org/10.1037/h0062126>
- Gray, J. A. (1982). *The neuropsychology of anxiety: An enquiry into the functions of the septo-hippocampal system*. Clarendon Press/Oxford University Press.
- Haber, S. N. (2003). The primate basal ganglia: Parallel and integrative networks. *Journal of Chemical Neuroanatomy*, *26*(4), 317–330. <https://doi.org/10.1016/j.jchemneu.2003.10.003>
- Hamilton, D. A., & Brigman, J. L. (2015). Behavioral flexibility in rats and mice: Contributions of distinct frontocortical regions. *Genes, Brain and Behavior*, *14*, 4–21. <https://doi.org/10.1111/gbb.12191>
- Harris, K. D., Henze, D. A., Csicsvari, J., Hirase, H., & Buzsáki, G. (2000). Accuracy of tetrode spike separation as determined by simultaneous intracellular and extracellular measurements. *Journal of Neurophysiology*, *84*(1), 401–414. <https://doi.org/10.1152/jn.2000.84.1.401>
- Hasselmo, M. E. (2005). A model of prefrontal cortical mechanisms for goal-directed behavior. *Journal of Cognitive Neuroscience*, *17*(7), 1115–1129. <https://doi.org/10.1162/0898929054475190>
- Hazan, L., Zugaro, M. B., & Buzsáki, G. (2006). Klusters, NeuroScope, NDManager: A free software suite for neurophysiological data processing and visualization. *Journal of Neuroscience Methods*, *155*, 207–216. <https://doi.org/10.1016/j.jneumeth.2006.01.017>
- Holroyd, C. B., & McClure, S. M. (2015). Hierarchical control over effortful behavior by rodent medial frontal cortex: A computational model. *Psychological Review*, *122*(1), 54–83. <https://doi.org/10.1037/a0038339>
- Hyman, J. M., Hasselmo, M. E., & Seamans, J. K. (2011). What is the functional relevance of prefrontal cortex entrainment to hippocampal theta rhythms? *Frontiers in Neuroscience*, *5*, 24. <https://doi.org/10.3389/fnins.2011.00024>
- Hyman, J. M., Holroyd, C. B., & Seamans, J. K. (2017). A novel neural prediction error found in anterior cingulate cortex ensembles. *Neuron*, *95*(2), 447–456.e3. <https://doi.org/10.1016/j.neuron.2017.06.021>
- Hyman, J. M., Zilli, E. A., Paley, A. M., & Hasselmo, M. E. (2005). Medial prefrontal cortex cells show dynamic modulation with the hippocampal theta rhythm dependent on behavior. *Hippocampus*, *15*, 739–749. <https://doi.org/10.1002/hipo.20106>
- Jadhav, S. P., Rothschild, G., Roumis, D. K., & Frank, L. M. (2016). Coordinated excitation and inhibition of prefrontal ensembles during awake hippocampal sharp-wave ripple events. *Neuron*, *90*(1), 113–127. <https://doi.org/10.1016/j.neuron.2016.02.010>

- Jay, T. M., & Witter, M. P. (1991). Distribution of hippocampal CA1 and subicular efferents in the prefrontal cortex of the rat studied by means of anterograde transport of Phaseolus vulgaris-leucoagglutinin. *The Journal of Comparative Neurology*, 313(4), 574–586. <https://doi.org/10.1002/cne.903130404>
- Jones, M. W., & Wilson, M. A. (2005). Theta rhythms coordinate hippocampal–prefrontal interactions in a spatial memory task. *PLoS Biology*, 3(12), e402. <https://doi.org/10.1371/journal.pbio.0030402>
- Jung, M. W., Qin, Y., Lee, D., & McNaughton, B. L. (1998). Firing characteristics of deep layer neurons in prefrontal cortex in rats performing spatial working memory tasks. *Cerebral Cortex*, 8, 437–450. <https://doi.org/10.1093/cercor/8.5.437>
- Kaefer, K., Nardin, M., Blahna, K., & Csicsvari, J. (2020). Replay of behavioral sequences in the medial prefrontal cortex during rule switching. *Neuron*, 106(1), 154–165.e6. <https://doi.org/10.1016/j.neuron.2020.01.015>
- Kafkas, A., & Montaldi, D. (2018). How do memory systems detect and respond to novelty? *Neuroscience Letters*, 680, 60–68. <https://doi.org/10.1016/j.neulet.2018.01.053>
- Kargo, W. J., Szatmary, B., & Nitz, D. A. (2007). Adaptation of prefrontal cortical firing patterns and their fidelity to changes in action-reward contingencies. *The Journal of Neuroscience*, 27(13), 3548–3559. <https://doi.org/10.1523/JNEUROSCI.3604-06.2007>
- Karlsson, M. P., Tervo, D. G., & Karpova, A. Y. (2012). Network resets in medial prefrontal cortex mark the onset of behavioral uncertainty. *Science*, 338(6103), 135–139. <https://doi.org/10.1126/science.1226518>
- Khamassi, M., & Humphries, M. D. (2012). Integrating cortico-limbic-basal ganglia architectures for learning model-based and model-free navigation strategies. *Frontiers in Behavioral Neuroscience*, 6, 79. <https://doi.org/10.3389/fnbeh.2012.00079>
- Khamassi, M., Quilodran, R., Enel, P., Dominey, P. F., & Procyk, E. (2015). Behavioral regulation and the modulation of information coding in the lateral prefrontal and cingulate cortex. *Cerebral Cortex*, 25(9), 3197–3218. <https://doi.org/10.1093/cercor/bhu114>
- Killcross, A. S., & Coutureau, E. (2003). Coordination of actions and habits in the medial prefrontal cortex of rats. *Cerebral Cortex*, 13(4), 400–408. <https://doi.org/10.1093/cercor/13.4.400>
- Kumaran, D., & Maguire, E. A. (2006). An unexpected sequence of events: Mismatch detection in the human hippocampus. *PLoS Biology*, 4(12), e424. <https://doi.org/10.1371/journal.pbio.0040424>
- Lansink, C. S., Goltstein, P. M., Lankelma, J. V., McNaughton, B. L., & Pennartz, C. M. (2009). Hippocampus leads ventral striatum in replay of place-reward information. *PLoS Biology*, 7(8), e1000173. <https://doi.org/10.1371/journal.pbio.1000173>
- Lapiz, M. D., & Morilak, D. A. (2006). Noradrenergic modulation of cognitive function in rat medial prefrontal cortex as measured by attentional set shifting capability. *Neuroscience*, 137(3), 1039–1049. <https://doi.org/10.1016/j.neuroscience.2005.09.031>
- Lapiz-Bluhm, M. D., Soto-Piña, A. E., Hensler, J. G., & Morilak, D. A. (2009). Chronic intermittent cold stress and serotonin depletion induce deficits of reversal learning in an attentional set-shifting test in rats. *Psychopharmacol (Berl)*, 202(1–3), 329–341. <https://doi.org/10.1007/s00213-008-1224-6>
- Lenartowicz, A., & McIntosh, A. R. (2005). The role of anterior cingulate cortex in working memory is shaped by functional connectivity. *Journal of Cognitive Neuroscience*, 17(7), 1026–1042. <https://doi.org/10.1162/0898929054475127>
- Li, L., & Shao, J. (1998). Restricted lesions to ventral prefrontal subareas block reversal learning but not visual discrimination learning in rats. *Physiology & Behavior*, 65, 371–379. [https://doi.org/10.1016/S0031-9384\(98\)00216-9](https://doi.org/10.1016/S0031-9384(98)00216-9)
- Lindsay, A. J., Caracheo, B. F., Grewal, J. J. S., Leibovitz, D., & Seamans, J. K. (2018). How much does movement and location encoding impact prefrontal cortex activity? An algorithmic decoding approach in freely moving rats. *eNeuro*, 5(2) pii: ENEURO.0023-18.2018. <https://doi.org/10.1523/ENEURO.0023-18.2018>
- Maingret, N., Girardeau, G., Todorova, R., Goutierre, M., & Zugaro, M. (2016). Hippocampo-cortical coupling mediates memory consolidation during sleep. *Nature Neuroscience*, 19(7), 959–964. <https://doi.org/10.1038/nn.4304>
- Malagon-Vina, H., Ciocchi, S., Passecker, J., Dorffner, G., & Klausberger, T. (2018). Fluid network dynamics in the prefrontal cortex during multiple strategy switching. *Nature Communications*, 9(1), 309. <https://doi.org/10.1038/s41467-017-02764-x>
- Malenka, R. C., Nestler, E. J., & Hyman, S. E. (2009). Chapter 13: Higher cognitive function and behavioral control. In A. Sydor & R. Y. Brown (Eds.), *Molecular neuropharmacology: A foundation for clinical neuroscience* (2nd ed.) (pp. 313–321). McGraw-Hill Medical. ISBN 978-0-07-148127-4
- Mansouri, F. A., Matsumoto, K., & Tanaka, K. (2006). Prefrontal cell activities related to monkeys' success and failure in adapting to rule changes in a Wisconsin card sorting test analog. *The Journal of Neuroscience*, 26(10), 274556. <https://doi.org/10.1523/JNEUROSCI.5238-05.2006>
- Martinet, L. E., Sheynikhovich, D., Benchenane, K., & Arleo, A. (2011). Spatial learning and action planning in a prefrontal cortical network model. *PLoS Computational Biology*, 7(5), e1002045. <https://doi.org/10.1371/journal.pcbi.1002045>
- Michon, F., Sun, J. J., Kim, C. Y., Ciliberti, D., & Kloosterman, F. (2019). Post-learning hippocampal replay selectively reinforces spatial memory for highly rewarded locations. *Current Biology*, 29(9), 1436–1444.e5. <https://doi.org/10.1016/j.cub.2019.03.048>
- Milner, B. (1963). Effects of different brain lesions on card sorting. *Archives of Neurology*, 9, 90–100. <https://doi.org/10.1001/archneur.1963.00460070100010>
- Miyazaki, K., Miyazaki, K. W., & Matsumoto, G. (2004). Different representation of forthcoming reward in nucleus accumbens and medial prefrontal cortex. *Neuroreport*, 15(4), 721–726. <https://doi.org/10.1097/00001756-200403220-00030>
- Mulder, A. B., Nordquist, R. E., Orgut, O., & Pennartz, C. M. (2003). Learning-related changes in response patterns of prefrontal neurons during instrumental conditioning. *Behavioural Brain Research*, 146(12), 77–88. <https://doi.org/10.1016/j.bbr.2003.09.016>
- O'Keefe, J. (1976). Place units in the hippocampus of the freely moving rat. *Experimental Neurology*, 51(1), 78–109. [https://doi.org/10.1016/0014-4886\(76\)90055-8](https://doi.org/10.1016/0014-4886(76)90055-8)
- O'Neill, P. K., Gordon, J. A., & Sigurdsson, T. (2013). Theta oscillations in the medial prefrontal cortex are modulated by spatial working memory and synchronize with the hippocampus

- through its ventral subregion. *The Journal of Neuroscience*, 33(35), 14211–14224. <https://doi.org/10.1523/JNEUROSCI.2378-13.2013>
- Peyrache, A., Khamassi, M., Benchenane, K., Wiener, S. I., & Battaglia, F. P. (2009). Replay of rule-learning related neural patterns in the prefrontal cortex during sleep. *Nature Neuroscience*, 12(7), 919–926. <https://doi.org/10.1038/nn.2337>
- Poucet, B. (1997). Searching for spatial unit firing in the prelimbic area of the rat medial prefrontal cortex. *Behavioural Brain Research*, 84, 151–159. [https://doi.org/10.1016/S0166-4328\(96\)00144-1](https://doi.org/10.1016/S0166-4328(96)00144-1)
- Powell, N. J., & Redish, A. D. (2016). Representational changes of latent strategies in rat medial prefrontal cortex precede changes in behaviour. *Nature Communications*, 7, 12830. <https://doi.org/10.1038/ncomms12830>
- Pratt, W. E., & Mizumori, S. J. (2001). Neurons in rat medial prefrontal cortex show anticipatory rate changes to predictable differential rewards in a spatial memory task. *Behavioural Brain Research*, 123(2), 165–183. [https://doi.org/10.1016/S0166-4328\(01\)00204-2](https://doi.org/10.1016/S0166-4328(01)00204-2)
- Procyk, E., & Goldman-Rakic, P. S. (2006). Modulation of dorsolateral prefrontal delay activity during self-organized behavior. *The Journal of Neuroscience*, 26(44), 11313–11323. <https://doi.org/10.1523/JNEUROSCI.2157-06.2006>
- Ragozzino, M. E., Detrick, S., & Kesner, R. P. (1999). Involvement of the prelimbic-infralimbic areas of the rodent prefrontal cortex in behavioral flexibility for place and response learning. *The Journal of Neuroscience*, 19(11), 4585–4594. <https://doi.org/10.1523/JNEUROSCI.19-11-04585.1999>
- Ragozzino, M. E., Wilcox, C., Raso, M., & Kesner, R. P. (1999). Involvement of rodent prefrontal cortex subregions in strategy switching. *Behavioral Neuroscience*, 113(1), 32–41. <https://doi.org/10.1037/0735-7044.113.1.32>
- Ramadan, W., Eschenko, O., & Sara, S. J. (2009). Hippocampal sharp wave/ripples during sleep for consolidation of associative memory. *PLoS ONE*, 4(8), e6697. <https://doi.org/10.1371/journal.pone.0006697>
- Raudies, F., & Hasselmo, M. E. (2014). A model of hippocampal spiking responses to items during learning of a context-dependent task. *Frontiers in Systems Neuroscience*, 8, 178. <https://doi.org/10.3389/fnsys.2014.00178>
- Rich, E. L., & Shapiro, M. (2009). Rat prefrontal cortical neurons selectively code strategy switches. *The Journal of Neuroscience*, 29(22), 7208–7219. <https://doi.org/10.1523/JNEUROSCI.6068-08.2009>
- Robbins, T. W. (2007). Shifting and stopping: Fronto-striatal substrates, neurochemical modulation and clinical implications. *Philosophical Transactions of the Royal Society B: Biological Sciences*, 362(1481), 917–932. <https://doi.org/10.1098/rstb.2007.2097>
- Rothschild, G., Eban, E., & Frank, L. M. (2017). A cortical–hippocampal–cortical loop of information processing during memory consolidation. *Nature Neuroscience*, 20(2), 251–259. <https://doi.org/10.1038/nn.4457>
- Roux, L., Hu, B., Eichler, R., Stark, E., & Buzsáki, G. (2017). Sharp wave ripples during learning stabilize the hippocampal spatial map. *Nature Neuroscience*, 20(6), 845–853. <https://doi.org/10.1038/nn.4543>
- Salazar, R. F., White, W., Lacroix, L., Feldon, J., & White, I. M. (2004). NMDA lesions in the medial prefrontal cortex impair the ability to inhibit responses during reversal of a simple spatial discrimination. *Behavioural Brain Research*, 152(2), 413–424. <https://doi.org/10.1016/j.bbr.2003.10.034>
- Seo, H., & Lee, D. (2009). Behavioral and neural changes after gains and losses of conditioned reinforcers. *The Journal of Neuroscience*, 29(11), 3627–3641. <https://doi.org/10.1523/JNEUROSCI.4726-08.2009>
- Shallice, T. (1988). *From neuropsychology to mental structure*. Cambridge University Press. <https://doi.org/10.1017/CBO9780511526817>
- Siapas, A. G., Lubenov, E. V., & Wilson, M. A. (2005). Prefrontal phase locking to hippocampal theta oscillations. *Neuron*, 46, 141–151. <https://doi.org/10.1016/j.neuron.2005.02.028>
- Skaggs, W. E., McNaughton, B. L., Wilson, M. A., & Barnes, C. A. (1996). Theta phase precession in hippocampal neuronal populations and the compression of temporal sequences. *Hippocampus*, 6(2), 149–172. [https://doi.org/10.1002/\(sici\)1098-1063\(1996\)6:2<149::aid-hipo6>3.0.co;2-k](https://doi.org/10.1002/(sici)1098-1063(1996)6:2<149::aid-hipo6>3.0.co;2-k)
- Tabuchi, E., Mulder, A. B., & Wiener, S. I. (2003). Reward value invariant place responses and reward site associated activity in hippocampal neurons of behaving rats. *Hippocampus*, 13(1), 117–132. <https://doi.org/10.1002/hipo.10056>
- Tait, D. S., Phillips, J. M., Blackwell, A. D., & Brown, V. J. (2017). Effects of lesions of the subthalamic nucleus/zona incerta area and dorsomedial striatum on attentional set-shifting in the rat. *Neuroscience*, 345, 287–296. <https://doi.org/10.1016/j.neuroscience.2016.08.008>
- Tanaka, S. (2007). Stable and unstable activation of the prefrontal cortex with dopaminergic modulation. Pps. In K. Y. Tseng & M. Atzori (Eds.), *Monoaminergic modulation of cortical excitability* (pp. 235–236). Springer. https://doi.org/10.1007/978-0-387-72256-6_16
- Tang, W., Shin, J. D., Frank, L. M., & Jadhav, S. P. (2017). Hippocampal-prefrontal reactivation during learning is stronger in awake compared with sleep states. *The Journal of Neuroscience*, 37(49), 11789–11805. <https://doi.org/10.1523/JNEUROSCI.2291-17.2017>
- Tatsuno, M., Malek, S., Kalvi, L., Ponce-Alvarez, A., Ali, K., Euston, D. R., Grün, S., & McNaughton, B. L. (2020). Memory reactivation in rat medial prefrontal cortex occurs in a subtype of cortical UP state during slow-wave sleep. *Philosophical Transactions of the Royal Society of London. Series B, Biological Sciences*, 375(1799), 20190227. <https://doi.org/10.1098/rstb.2019.0227>
- Thierry, A. M., Gioanni, Y., Dégénétais, E., & Glowinski, J. (2000). Hippocampo-prefrontal cortex pathway: anatomical and electrophysiological characteristics. *Hippocampus*, 10, 411–419. [https://doi.org/10.1002/1098-1063\(2000\)10:4<411::AID-HIPO7>3.0.CO;2-A](https://doi.org/10.1002/1098-1063(2000)10:4<411::AID-HIPO7>3.0.CO;2-A)
- Trouche, S., Koren, V., Doig, N. M., Ellender, T. J., el-Gaby, M., Lopes-dos-Santos, V., Reeve, H. M., Perestenko, P. V., Garas, F. N., Magill, P. J., Sharott, A., & Dupret, D. (2019). A hippocampus-accumbens tripartite neuronal motif guides appetitive memory in space. *Cell*, 176(6), 1393–1406.e16. <https://doi.org/10.1016/j.cell.2018.12.037>
- van Heukelum, S., Mars, R. B., Guthrie, M., Buitelaar, J. K., Beckmann, C. F., Tiesinga, P. H. E., Vogt, B. A., Glennon, J. C., & Havenith, M. N. (2020). Where is cingulate cortex? A cross-species view. *Trends in Neurosciences*, 43(5), 285–299. <https://doi.org/10.1016/j.tins.2020.03.007>

- Vinogradova, O. S. (2001). Hippocampus as comparator: Role of the two input and two output systems of the hippocampus in selection and registration of information. *Hippocampus*, *11*, 578–598. <https://doi.org/10.1002/hipo.1073>
- Wagatsuma, H., & Yamaguchi, Y. (2004). Cognitive map formation through sequence encoding by theta phase precession. *Neural Computation*, *16*, 2665–2697. <https://doi.org/10.1162/0899766042321742>
- Wang, M. Z., & Hayden, B. Y. (2017). Reactivation of associative structure specific outcome responses during prospective evaluation in reward-based choices. *Nature Communications*, *8*(1), 15821. <https://doi.org/10.1038/ncomms15821>
- Wierzynski, C. M., Lubenov, E. V., Gu, M., & Siapas, A. G. (2009). State-dependent spike-timing relationships between hippocampal and prefrontal circuits during sleep. *Neuron*, *61*(4), 587–596. <https://doi.org/10.1016/j.neuron.2009.01.011>
- Yu, J. Y., & Frank, L. M. (2015). Hippocampal-cortical interaction in decision making. *Neurobiology of Learning and Memory*, *117*, 34–41. <https://doi.org/10.1016/j.nlm.2014.02.002>
- Yu, J. Y., Kay, K., Liu, D. F., Grossrubatscher, I., Loback, A., Sosa, M., Chung, J. E., Karlsson, M. P., Larkin, M. C., & Frank, L. M. (2017). Distinct hippocampal-cortical memory representations for experiences associated with movement versus immobility. *eLife*, *6*, e27621. <https://doi.org/10.7554/eLife.27621>
- Yu, J. Y., Liu, D. F., Loback, A., Grossrubatscher, I., & Frank, L. M. (2018). Specific hippocampal representations are linked to generalized cortical representations in memory. *Nature Communications*, *9*(1), 2209. <https://doi.org/10.1038/s41467-018-04498-w>

SUPPORTING INFORMATION

Additional supporting information can be found online in the Supporting Information section at the end of this article.

How to cite this article: Khamassi, M., Peyrache, A., Benchenane, K., Hopkins, D. A., Lebas, N., Douchamps, V., Droulez, J., Battaglia, F. P., & Wiener, S. I. (2024). Rat anterior cingulate neurons responsive to rule or strategy changes are modulated by the hippocampal theta rhythm and sharp-wave ripples. *European Journal of Neuroscience*, 1–28. <https://doi.org/10.1111/ejn.16496>